Copy 542

[redacted]

NASA TM X-69

NASA TM X-69

[redacted]

[redacted]

TECHNICAL MEMORANDUM

GROUP (3)

[redacted]

X - 69

[redacted]

AN INVESTIGATION AT MACH NUMBERS FROM 1.47 TO 2.87 OF STATIC STABILITY CHARACTERISTICS OF NINE NOSE CONES DESIGNED FOR SUPERSONIC IMPACT VELOCITIES

By Donald T. Gregory and Ausley B. Carraway

Langley Research Center
Langley Field, Va.

CATEGORY
SPECIAL HANDLING
7

[redacted]

NATIONAL AERONAUTICS AND SPACE ADMINISTRATION
WASHINGTON September 1959

[redacted]

M

[redacted]

NATIONAL AERONAUTICS AND SPACE ADMINISTRATION

TECHNICAL MEMORANDUM X-69

AN INVESTIGATION AT MACH NUMBERS FROM 1.47 TO 2.87 OF STATIC STABILITY CHARACTERISTICS OF NINE NOSE CONES DESIGNED FOR SUPERSONIC IMPACT VELOCITIES*

By Donald T. Gregory and Ausley B. Carraway

L
3
5
6

SUMMARY

An investigation of nine nose cones designed for supersonic impact velocities has been conducted in the Langley Unitary Plan wind tunnel to determine the axial force and static longitudinal stability characteristics. These configurations are suitable for use as nose cones for either intermediate-range or intercontinental ballistic missiles. The model dimensional parameters that varied were nose shape and body flare length. One body incorporated flared fins.

Tests were performed at Mach numbers of 1.47, 1.97, 2.36, and 2.87 and at Reynolds numbers per foot from 0.7×10^6 to 8.6×10^6.

INTRODUCTION

Nose cones for intermediate-range and intercontinental ballistic missiles up to this time have been designed for subsonic impact velocities, primarily because of the high heat rates encountered by the cones during atmospheric reentry. An increase in the impact velocities of such configurations is desirable, since this will minimize the problems of dispersion and perhaps interception. Improvements in materials for nose-cone heat shields and accurate determination of heat-transfer coefficients have provided impetus for the design of supersonic impact warheads. Knowledge of the stability and drag characteristics of such configurations is, obviously, necessary in order that they may be fired at a target with a high degree of accuracy.

---

*[redacted]

[redacted]

The Langley Research Center of NASA has accordingly initiated a research program to determine static and dynamic stability characteristics of several basic configurations suitable for supersonic impact velocities. This program provides for tests of these configurations in several Langley facilities in the supersonic and hypersonic speed regime, and through a large Reynolds number range.

The present paper contains the results of tests in the Langley Unitary Plan wind tunnel to determine the axial force and the static longitudinal stability characteristics of nine configurations at Mach numbers of 1.47, 1.97, 2.36, and 2.87 and at Reynolds numbers per foot from 0.7×10^6 to 8.6×10^6. Angle of attack was varied from approximately -1° to 29°. The results are presented without analysis.

L
3
5
6

SYMBOLS

The aerodynamic force and moment data are referred to the body axes (fig. 1) with the origin at the center of gravity (fig. 2). Symbols used are defined as follows:

A_j cross-sectional area at juncture of nose and body (based on 4-in. diameter), sq ft

C_A axial-force coefficient, $\frac{\text{Axial force}}{qA_j}$

$C_{A,c}$ chamber axial-force coefficient, $\frac{\text{Chamber axial force}}{qA_j}$

C_m pitching-moment coefficient, $\frac{\text{Pitching moment}}{qA_j d_b}$

C_{m_α} slope of pitching-moment curve near $\alpha = 0^\circ$, $\frac{\partial C_m}{\partial \alpha}$

C_N normal-force coefficient, $\frac{\text{Normal force}}{qA_j}$

d_b base diameter, 6.072 in.

[redacted]

l_n	length of nose, in.
l_f	length of flare, in.
M	free-stream Mach number
q	free-stream dynamic pressure, lb/sq ft
R	Reynolds number per foot
L 3 α	angle of attack of model center line, deg

APPARATUS AND TESTS

Tunnel

Tests were conducted in the low Mach number test section of the Langley Unitary Plan wind tunnel, which is a variable-pressure, continuous-flow tunnel. The test section is 4 feet square and 7 feet long. The nozzle leading to the test section is of the asymmetric, sliding-block type, which permits a continuous variation in test section Mach number from about 1.47 to 2.87.

Models

Profile and rear-view drawings of the models tested are shown in figure 2. The models are identified as models 1 to 9 and, as may be noted from figure 2, have been divided into three families dependent on nose shape. The first family (models 1 to 4) had flat-face noses of circular cross section tapering from a diameter of 1.752 inches at the front to a diameter of 4.000 inches at a distance 3.084 inches from the front. The second family (models 5 to 7) had rounded noses of 1.372-inch nose radius, which faired into the body cross section (of 4.000-inch diameter) at a distance 2.492 inches from the front. The third family (models 8 and 9) also had flat-face noses tapering in diameter from 1.204 inches at the front to 4.000 inches at a distance 3.836 inches from the front. In each family, the body flare length varied from about 6 inches to 15 inches; in addition, one family included a model with a finned flare (model 4). In order to clarify further the dimensional characteristics of the models, the nose lengths l_n and flare lengths l_f are given as ratios with respect to the base diameter d_b (6.072 in.) as follows:

[redacted]

Model	Nose-length ratio, l_n/d_b	Flare-length ratio, l_f/d_b
1	0.51	2.52
2	.51	1.82
3	.51	.97
4	.51	2.52
5	.41	2.52
6	.41	1.82
7	.41	.97
8	.63	2.52
9	.63	.97

L
3
5
6

Test Conditions and Procedure

The tests were conducted at Mach numbers of 1.47, 1.97, 2.36, and 2.87 and at stagnation pressures that were varied in order to provide a constant test Reynolds number per foot of 3.5×10^6. In addition, at a Mach number of 1.97 the Reynolds number per foot was varied from 0.7×10^6 to 8.6×10^6. The dewpoint at stagnation pressure was maintained below -30° F in order to assure negligible condensation effects. Stagnation temperatures for the test were 125° F for Mach numbers 1.47 and 1.97 and 150° F for Mach numbers 2.36 and 2.87. The angle of attack was varied from approximately -1° to 29°, and sideslip angle was maintained near 0°.

All models incorporated a fixed transition strip 1 inch behind the forward end of the nose. This strip was composed of a band of 0.012 carborundum grain 1/32 inch wide.

Measurements

Aerodynamic forces and moments were determined by means of an internal six-component strain-gage balance housed within the model. The balance was rigidly fastened to the sting support system.

Balance chamber pressure was measured with a single static orifice located in the vicinity of the strain-gage balance.

Schlieren photographs of each of the models were taken at all test Mach numbers and at various model attitudes and test conditions.

[redacted]

Corrections

Calibration of the tunnel test section has indicated that model buoyancy effects are negligible. Corrections to the model angle of attack have been made for both tunnel airflow misalinement and deflection of model and sting support due to aerodynamic load.

The axial-force data presented herein have been adjusted to correspond to zero balance-chamber axial force. A listing of the chamber axial-force coefficients for the various models, Mach numbers, and Reynolds numbers is presented in table I.

L
3
5
6

Accuracy

Based upon balance calibration and repeatability of data, it is estimated that the various measured quantities are accurate within the following limits:

Quantity	$R = 0.7 \times 10^6$	$R = 3.5 \times 10^6$	$R = 8.6 \times 10^6$
C_A	±0.050	±0.010	±0.005
$C_{A,c}$	±0.014	±0.002	±0.001
C_m	±0.028	±0.004	±0.002
C_N	±0.150	±0.030	±0.015
α, deg	±0.1	±0.1	±0.1

The maximum deviation of the local Mach number from the free-stream value given is ±0.015.

PRESENTATION OF RESULTS

Schlieren Photographs

Typical schlieren photographs for the various models are presented in figure 3 for a Mach number of 2.87 at $\alpha \approx 0^\circ$. Schlieren photographs of model 7 with Mach number, Reynolds number, and angle of attack varied are shown in figures 4, 5, and 6, respectively.

Aerodynamic Characteristics

The aerodynamic characteristics for all models are presented in figures 7 to 15, where the coefficients of normal force C_N, axial force C_A, and pitching moment C_m are plotted against angle of attack. Mach number is used as a variable in the (a) parts of figures 7 to 15 and Reynolds number as a variable in the (b) parts of these figures. Figure 16 is a summary plot showing the pitching-moment slopes C_{m_α} and the drag levels $\left((C_A)_{\alpha=0^\circ}\right)$ for the different models as functions of Mach number.

L356

The following table is included for convenience in locating the figures containing the aerodynamic data for the various models:

In order to expedite publication of these data, no analysis is attempted.

CONCLUDING REMARKS

Aerodynamic data have been presented for nine nose-cone configurations designed for supersonic impact velocities. The model dimensional parameters were nose shape and body flare length. One body incorporated flared fins. The results presented herein include axial-force and longitudinal stability characteristics, and schlieren photographs at Mach numbers of 1.47, 1.97, 2.36, and 2.87 and at Reynolds numbers per foot from about 0.7×10^6 to 8.6×10^6.

Langley Research Center,
National Aeronautics and Space Administration,
Langley Field, Va., June 4, 1959.

[redacted]

TABLE I.- LISTING OF CHAMBER AXIAL-FORCE COEFFICIENTS FOR ALL TEST CONFIGURATIONS AT ALL MODEL ATTITUDES AND TEST CONDITIONS

(a) Model 1

$[R = 3.5 \times 10^6]$

M = 1.47		M = 1.97		M = 2.36		M = 2.87	
α, deg	$C_{A,c}$	α, deg	$C_{A,c}$	α, deg	$C_{A,c}$	α, deg	$C_{A,c}$
-0.43	0.3861	0.29	0.3043	0.62	0.2538	-0.81	0.2013
.54	.3857	1.28	.3118	1.59	.2652	.20	.1981
1.58	.3954	2.33	.3278	2.61	.2813	1.16	.1993
2.63	.4140	3.36	.3496	3.63	.3034	2.14	.2084
3.63	.4258	4.33	.3746	4.61	.3192	3.13	.2222
6.76	.5074	7.45	.4335	7.67	.3637	6.10	.2562
12.08	.6752	12.66	.5253	12.79	.4097	11.17	.2875
17.50	.7836	17.91	.5500	18.04	.4025	16.34	.2901
22.92	.7817	23.32	.5022	23.49	.3765	21.75	.2668
27.87	.7098	28.35	.4771	28.50	.3580	26.70	.2559

$[M = 1.97]$

R = 0.7 × 10^6		R = 2.1 × 10^6		R = 3.5 × 10^6		R = 4.9 × 10^6		R = 6.5 × 10^6		R = 8.6 × 10^6	
α, deg	$C_{A,c}$	α, deg	$C_{A,c}$	α, deg	$C_{A,c}$	α, deg	$C_{A,c}$	α, deg	$C_{A,c}$	α, deg	$C_{A,c}$
0.28	0.2980	0.30	0.2964	0.29	0.3043	0.34	0.3121	0.33	0.3198	0.34	0.3239
1.21	.3041	1.27	.3025	1.28	.3118	1.34	.3199	1.45	.3271	1.49	.3322
2.09	.3155	2.23	.3171	2.33	.3278	2.42	.3361	2.52	.3434	2.67	.3475
3.09	.3344	3.19	.3375	3.36	.3496	3.49	.3578	3.65	.3669	3.84	.3711
4.02	.3584	4.16	.3629	4.33	.3746	4.50	.3834	4.73	.3916	4.99	.3955
6.88	.4289	7.17	.4223	7.45	.4335	7.74	.4421	8.08	.4491	8.51	.4536
11.74	.5128	12.19	.5193	12.66	.5253	13.13	.5305	13.67	.5353	14.40	.5389
16.74	.5282	17.32	.5460	17.91	.5500	18.50	.5525	19.21	.5543	31.43	.4683
21.95	.4930	22.63	.5031	23.32	.5022	24.03	.4988	24.86	.4976	25.95	.4935
26.76	.4762	27.55	.4755	28.35	.4771	29.18	.4770	30.14	.4752	20.13	.5523

TABLE I.- LISTING OF CHAMBER AXIAL-FORCE COEFFICIENTS FOR ALL TEST CONFIGURATIONS

AT ALL MODEL ATTITUDES AND TEST CONDITIONS - Continued

(b) Model 2

$\left[R = 3.5 \times 10^6\right]$

M = 1.47		M = 1.97		M = 2.36		M = 2.87	
α, deg	$C_{A,c}$	α, deg	$C_{A,c}$	α, deg	$C_{A,c}$	α, deg	$C_{A,c}$
-0.43	0.4086	0.32	0.3200	0.63	0.2691	-0.78	0.2157
.52	.4115	1.26	.3254	1.56	.2780	.21	.2131
1.54	.4167	2.24	.3371	2.57	.2919	1.16	.2140
2.57	.4325	3.27	.3579	3.57	.3095	2.15	.2203
3.52	.4473	4.26	.3796	4.54	.3271	3.10	.2325
6.59	.5189	7.30	.4383	7.52	.3653	6.05	.2635
11.83	.6629	12.46	.5256	12.59	.4113	11.02	.2890
17.21	.7709	17.65	.5489	17.74	.4073	16.12	.2932
22.59	.7732	22.99	.5048	23.14	.3779	21.46	.2732
27.50	.7211	27.93	.4808	28.02	.3620	26.31	.2598

$\left[M = 1.97\right]$

$R = 0.7 \times 10^6$		$R = 2.1 \times 10^6$		$R = 3.5 \times 10^6$		$R = 4.9 \times 10^6$		$R = 6.5 \times 10^6$		$R = 8.6 \times 10^6$	
α, deg	$C_{A,c}$	α, deg	$C_{A,c}$	α, deg	$C_{A,c}$	α, deg	$C_{A,c}$	α, deg	$C_{A,c}$	α, deg	$C_{A,c}$
0.26	0.3056	0.30	0.3085	0.32	0.3200	0.33	0.3287	0.32	0.3361	0.34	0.3424
1.17	.3146	1.22	.3142	1.26	.3254	1.31	.3344	1.42	.3434	1.44	.3485
2.13	.3248	2.20	.3254	2.24	.3371	2.36	.3480	2.45	.3547	2.57	.3631
3.08	.3387	3.16	.3447	3.27	.3579	3.38	.3666	3.54	.3755	3.68	.3814
3.98	.3630	4.12	.3657	4.26	.3796	4.43	.3897	4.55	.3955	4.78	.4042
6.87	.4336	7.10	.4260	7.30	.4383	7.57	.4475	7.81	.4533	8.21	.4603
11.70	.5128	12.07	.5187	12.46	.5236	12.85	.5304	13.30	.5343	13.90	.5404
16.69	.5455	17.16	.5470	17.65	.5489	18.13	.5533	18.71	.5569	19.47	.5603
21.88	.4999	22.44	.4994	22.99	.5048	23.57	.5050	24.23	.5009	25.12	.4964
26.67	.4821	27.30	.4793	27.93	.4808	28.57	.4802	29.32	.4789	30.30	.4765

[redacted]

TABLE I.- LISTING OF CHAMBER AXIAL-FORCE COEFFICIENTS FOR ALL TEST CONFIGURATIONS

AT ALL MODEL ATTITUDES AND TEST CONDITIONS - Continued

(c) Model 3

$\left[R = 3.5 \times 10^6\right]$

M = 1.47		M = 1.97		M = 2.36		M = 2.87	
α, deg	$C_{A,c}$	α, deg	$C_{A,c}$	α, deg	$C_{A,c}$	α, deg	$C_{A,c}$
-0.45	0.4547	0.29	0.3532	0.62	0.3034	-0.74	0.2412
.57	.4556	1.26	.3585	1.58	.3073	.21	.2420
1.52	.4606	2.26	.3657	2.50	.3146	1.15	.2421
2.53	.4672	3.25	.3790	3.54	.3280	2.13	.2430
3.51	.4826	4.26	.3968	4.47	.3395	3.08	.2465
6.51	.5406	7.28	.4526	7.47	.3729	5.99	.2662
11.76	.6646	12.39	.5193	12.49	.4002	10.93	.2927
17.16	.7438	17.55	.5517	17.61	.4282	16.00	.3017
22.56	.7970	22.84	.5453	22.93	.4041	21.27	.2784
27.45	.8264	27.72	.5086	27.76	.3684	26.06	.2623

$\left[M = 1.97\right]$

$R = 0.7 \times 10^6$		$R = 2.1 \times 10^6$		$R = 3.5 \times 10^6$		$R = 4.9 \times 10^6$		$R = 6.5 \times 10^6$		$R = 8.6 \times 10^6$	
α, deg	$C_{A,c}$	α, deg	$C_{A,c}$	α, deg	$C_{A,c}$	α, deg	$C_{A,c}$	α, deg	$C_{A,c}$	α, deg	$C_{A,c}$
0.29	0.3378	0.30	0.3416	0.29	0.3532	0.33	0.3640	0.35	0.3715	0.38	0.3767
1.21	.3392	1.25	.3454	1.26	.3585	1.34	.3681	1.39	.3762	1.46	.3809
2.12	.3449	2.20	.3524	2.26	.3657	2.34	.3758	2.41	.3835	2.54	.3894
3.08	.3563	3.18	.3657	3.25	.3790	3.38	.3890	3.50	.3964	3.65	.4016
4.00	.3753	4.13	.3829	4.26	.3968	4.36	.4052	4.53	.4119	4.74	.4193
6.86	.4409	7.05	.4405	7.28	.4526	7.48	.4614	7.75	.4670	8.09	.4727
11.69	.5099	12.05	.5133	12.39	.5193	12.75	.5250	13.17	.5292	13.72	.5340
16.67	.5407	17.11	.5487	17.55	.5517	18.00	.5536	18.54	.5553	19.22	.5569
21.86	.5255	22.36	.5422	22.84	.5453	23.36	.5475	23.97	.5443	24.73	.5438
26.63	.4906	27.19	.5163	27.72	.5086	28.30	.4970	28.96	.4908	29.79	.4872

[redacted]

[redacted]

TABLE I.- LISTING OF CHAMBER AXIAL-FORCE COEFFICIENTS FOR ALL TEST CONFIGURATIONS

AT ALL MODEL ATTITUDES AND TEST CONDITIONS - Continued

(d) Model 4

$\left[R = 3.5 \times 10^6\right]$

M = 1.47		M = 1.97		M = 2.36		M = 2.87	
α, deg	$C_{A,c}$	α, deg	$C_{A,c}$	α, deg	$C_{A,c}$	α, deg	$C_{A,c}$
-0.48	0.2864	0.31	0.2307	0.60	0.1955	-0.76	0.1505
.52	.2842	1.31	.2295	1.60	.1964	.21	.1521
1.56	.2885	2.26	.2371	2.60	.1947	1.16	.1511
2.60	.3032	3.33	.2383	3.61	.1953	2.15	.1499
3.58	.3136	4.30	.2418	4.59	.1989	3.13	.1496
6.68	.3496	7.38	.2641	7.61	.2148	6.09	.1551
11.94	.3873	12.51	.2811	12.67	.2208	11.09	.1603
17.28	.4153	17.78	.2829	17.93	.2258	16.27	.1598
22.82	.4461	23.24	.3044	23.41	.2259	21.69	.1581
27.92	.4286	28.26	.2890	28.39	.2133	26.62	.1509

$[M = 1.97]$

$R = 0.7 \times 10^6$		$R = 2.1 \times 10^6$		$R = 3.5 \times 10^6$		$R = 4.9 \times 10^6$		$R = 6.5 \times 10^6$		$R = 8.6 \times 10^6$	
α, deg	$C_{A,c}$	α, deg	$C_{A,c}$	α, deg	$C_{A,c}$	α, deg	$C_{A,c}$	α, deg	$C_{A,c}$	α, deg	$C_{A,c}$
0.28	0.2269	0.29	0.2261	0.31	0.2307	0.29	0.2345	0.35	0.2378	0.36	0.2408
1.16	.2267	1.26	.2247	1.31	.2295	1.36	.2334	1.43	.2374	1.50	.2403
2.12	.2295	2.21	.2319	2.26	.2371	2.39	.2407	2.50	.2442	2.63	.2466
3.09	.2308	3.18	.2331	3.33	.2383	3.46	.2419	3.61	.2448	3.79	.2469
3.98	.2372	4.17	.2369	4.30	.2418	4.49	.2447	4.68	.2475	4.93	.2496
6.87	.2600	7.13	.2588	7.38	.2641	7.66	.2684	7.97	.2719	8.37	.2751
11.71	.2754	12.10	.2783	12.51	.2811	12.93	.2837	13.42	.2859	14.06	.2876
16.70	.2645	17.24	.2768	17.78	.2829	18.32	.2861	18.99	.2884	19.85	.2898
21.91	.2909	22.60	.3051	23.24	.3044	23.95	.3050	24.76	.3047	25.81	.3026
26.74	.2808	27.50	.2877	28.26	.2890	29.06	.2876	30.01	.2853	31.21	.2821

[redacted]

TABLE I.- LISTING OF CHAMBER AXIAL-FORCE COEFFICIENTS FOR ALL TEST CONFIGURATIONS

AT ALL MODEL ATTITUDES AND TEST CONDITIONS - Continued

(e) Model 5

[$R = 3.5 \times 10^6$]

M = 1.47		M = 1.97		M = 2.36		M = 2.87	
α, deg	$C_{A,c}$	α, deg	$C_{A,c}$	α, deg	$C_{A,c}$	α, deg	$C_{A,c}$
-1.63	0.4886	-0.85	0.3537	-0.47	0.2850	-1.87	0.2241
-.58	.4708	.15	.3495	.53	.2830	-.87	.2248
.43	.4723	1.17	.3570	1.54	.2875	.14	.2218
1.41	.4884	2.14	.3684	2.51	.2964	1.11	.2204
2.47	.5104	3.20	.3822	3.57	.3066	2.16	.2241
5.51	.5454	6.24	.4208	6.60	.3395	5.18	.2389
10.69	.6756	11.43	.5218	11.79	.3945	10.33	.2740
15.77	.8168	16.51	.5772	16.85	.4285	15.37	.2969
20.97	.8835	21.69	.5770	22.02	.4268	20.49	.3023
26.27	.8122	26.95	.5639	27.26	.4238	25.71	.3006

[$M = 1.97$]

$R = 0.7 \times 10^6$		$R = 2.1 \times 10^6$		$R = 3.5 \times 10^6$		$R = 4.9 \times 10^6$		$R = 6.5 \times 10^6$		$R = 8.6 \times 10^6$	
α, deg	$C_{A,c}$	α, deg	$C_{A,c}$	α, deg	$C_{A,c}$	α, deg	$C_{A,c}$	α, deg	$C_{A,c}$	α, deg	$C_{A,c}$
-0.84	0.3349	-0.84	0.3451	-0.85	0.3537	-0.86	0.3613	-0.88	0.3674	-0.89	0.3777
.15	.3378	.15	.3426	.15	.3495	.15	.3574	.14	.3637	.14	.3767
1.14	.3408	1.15	.3491	1.17	.3570	1.18	.3650	1.19	.3706	1.20	.3782
2.09	.3502	2.12	.3555	2.14	.3684	2.17	.3754	2.18	.3816	2.20	.3844
3.13	.3585	3.16	.3701	3.20	.3822	3.23	.3891	3.26	.3936	3.30	.3960
6.12	.3844	6.18	.4002	6.24	.4208	6.30	.4279	6.37	.4305	6.46	.4311
11.19	.4293	11.32	.5020	11.43	.5218	11.55	.5112	11.68	.5233	11.87	.4690
16.14	.4916	16.32	.5588	16.51	.5772	16.71	.5800	16.91	.5850	17.21	.4926
21.18	.5166	21.43	.5663	21.69	.5770	21.96	.5786	22.25	.5786	22.65	.4967
26.30	.5245	26.62	.5611	26.95	.5639	27.29	.5616	27.67	.5606	28.20	.5602

[redacted]

TABLE I.- LISTING OF CHAMBER AXIAL-FORCE COEFFICIENTS FOR ALL TEST CONFIGURATIONS AT ALL MODEL ATTITUDES AND TEST CONDITIONS - Continued

(f) Model 6

$\left[R = 3.5 \times 10^6\right]$

M = 1.47		M = 1.97		M = 2.36		M = 2.87	
α, deg	$C_{A,c}$	α, deg	$C_{A,c}$	α, deg	$C_{A,c}$	α, deg	$C_{A,c}$
-1.63	0.5055	-0.85	0.3632	-----	------	-1.86	0.2298
-.58	.4937	.25	.3635	-----	------	-.86	.2332
.43	.4970	1.17	.3667	-----	------	.14	.2291
1.40	.5086	2.13	.3765	-----	------	1.11	.2293
2.45	.5276	3.19	.3893	-----	------	2.15	.2328
5.49	.5651	6.22	.4243	-----	------	5.17	.2472
10.65	.6789	11.40	.5095	-----	------	10.31	.2727
15.71	.8028	16.46	.5758	-----	------	15.33	.2872
20.90	.8632	21.63	.5695	-----	------	20.44	.2976
26.18	.8275	26.87	.5566	-----	------	25.66	.3013

L356

[redacted]

TABLE I.- LISTING OF CHAMBER AXIAL-FORCE COEFFICIENTS FOR ALL TEST CONFIGURATIONS AT ALL MODEL ATTITUDES AND TEST CONDITIONS - Continued

(g) Model 7

$[R = 3.5 \times 10^6]$

M = 1.47		M = 1.97		M = 2.36		M = 2.87	
α, deg	$C_{A,c}$	α, deg	$C_{A,c}$	α, deg	$C_{A,c}$	α, deg	$C_{A,c}$
-1.62	0.5526	-0.84	0.3967	-0.51	0.3142	-1.85	0.2460
-.58	.5487	.15	.3965	.53	.3153	-.85	.2436
.43	.5515	1.17	.4003	1.53	.3183	.15	.2414
1.40	.5616	2.13	.4083	2.50	.3231	1.11	.2415
2.45	.5763	3.18	.4150	3.55	.3283	2.13	.2442
5.47	.6079	6.22	.4420	6.58	.3508	5.17	.2607
10.64	.6871	11.38	.4975	11.74	.3883	10.29	.2812
15.69	.7829	16.45	.5685	16.79	.4370	15.33	.3079
20.86	.8753	21.59	.5905	21.92	.4571	20.44	.3150
26.13	.9374	26.82	.6093	27.14	.4409	25.62	.3113

$[M = 1.97]$

$R = 0.7 \times 10^6$		$R = 2.1 \times 10^6$		$R = 3.5 \times 10^6$		$R = 4.9 \times 10^6$		$R = 6.5 \times 10^6$		$R = 8.6 \times 10^6$	
α, deg	$C_{A,c}$	α, deg	$C_{A,c}$	α, deg	$C_{A,c}$	α, deg	$C_{A,c}$	α, deg	$C_{A,c}$	α, deg	$C_{A,c}$
-0.84	0.3642	-0.83	0.3879	-0.84	0.3967	-0.85	0.4037	-0.87	0.4091	0.15	0.5066
.24	.3691	.16	.3870	.15	.3965	.15	.4028	.15	.4080	1.20	.4864
1.14	.3748	1.16	.3902	1.17	.4003	1.17	.4073	1.17	.4119	2.19	.4662
2.09	.3838	2.12	.3963	2.13	.4083	2.14	.4143	2.16	.4193	3.27	.4431
3.12	.3906	3.16	.4039	3.18	.4150	3.21	.4223	3.23	.4270	6.39	.4459
6.11	.4191	6.17	.4309	6.22	.4420	6.26	.4504	6.31	.4559	11.72	.4586
11.18	.4530	11.29	.4846	11.38	.4975	11.47	.5060	22.06	.5971	17.01	.5086
16.13	.5115	16.29	.5520	16.45	.5685	16.59	.5776	27.42	.5937	22.38	.5465
21.16	.5340	21.38	.5945	21.59	.5805	21.81	.5917	-----	------	27.85	.5807
26.28	.5362	26.55	.6101	26.82	.6093	27.09	.6032	-----	------	-----	------

TABLE I.- LISTING OF CHAMBER AXIAL-FORCE COEFFICIENTS FOR ALL TEST CONFIGURATIONS AT ALL MODEL ATTITUDES AND TEST CONDITIONS - Continued

(h) Model 8

$[R = 3.5 \times 10^6]$

M = 1.47		M = 1.97		M = 2.36		M = 2.87	
α, deg	$C_{A,c}$	α, deg	$C_{A,c}$	α, deg	$C_{A,c}$	α, deg	$C_{A,c}$
-1.81	0.4009	-1.00	0.3060	-0.67	0.2534	-2.07	0.2129
-.68	.3882	.12	.3042	.40	.2522	-.99	.2038
.41	.3851	1.21	.3111	1.47	.2617	.08	.1945
1.61	.3978	2.36	.3305	2.67	.2830	1.21	.1947
2.66	.4160	3.43	.3539	3.71	.3038	2.25	.2057
5.99	.4932	6.73	.4256	6.99	.3571	5.45	.2524
11.51	.6722	12.20	.5317	12.37	.4165	10.77	.2884
17.02	.8106	17.55	.5819	17.72	.4229	16.06	.2978
22.36	.8619	22.89	.5507	23.09	.4139	21.38	.2907
27.26	.7904	27.84	.5493	28.07	.4069	26.27	.2874

$[M = 1.97]$

$R = 0.7 \times 10^6$		$R = 2.1 \times 10^6$		$R = 3.5 \times 10^6$		$R = 4.9 \times 10^6$		$R = 6.5 \times 10^6$		$R = 8.6 \times 10^6$	
α, deg	$C_{A,c}$	α, deg	$C_{A,c}$	α, deg	$C_{A,c}$	α, deg	$C_{A,c}$	α, deg	$C_{A,c}$	α, deg	$C_{A,c}$
-0.93	0.2948	-0.96	0.2954	-1.00	0.3060	-1.04	0.3144	-1.12	0.3221	-1.20	0.3287
.10	.2925	.11	.2934	.12	.3042	.12	.3122	.14	.3195	.15	.3255
1.06	.2998	1.15	.3003	1.21	.3111	1.26	.3192	1.33	.3269	1.39	.3331
2.16	.3157	2.26	.3169	2.36	.3305	2.46	.3400	2.58	.3478	2.72	.3538
3.15	.3346	3.29	.3405	3.43	.3539	3.58	.3639	3.75	.3721	3.95	.3791
6.20	.4318	6.46	.4120	6.73	.4256	6.99	.4363	7.31	.4433	7.70	.4515
11.28	.5363	11.73	.5245	12.20	.5317	12.66	.5375	13.23	.5434	13.95	.5498
16.34	.5769	16.95	.5745	17.55	.5819	18.18	.5857	18.91	.5892	19.88	.5907
21.45	.5334	22.17	.5474	22.89	.5507	23.65	.5502	24.53	.5504	25.68	.5515
26.16	.5276	26.99	.5377	27.84	.5493	28.73	.5488	29.78	.5482	31.14	.5499

TABLE I.- LISTING OF CHAMBER AXIAL-FORCE COEFFICIENTS FOR ALL TEST CONFIGURATIONS AT ALL MODEL ATTITUDES AND TEST CONDITIONS - Concluded

(i) Model 9

$\left[R = 3.5 \times 10^6\right]$

M = 1.47		M = 1.97		M = 2.36		M = 2.87	
α, deg	$C_{A,c}$	α, deg	$C_{A,c}$	α, deg	$C_{A,c}$	α, deg	$C_{A,c}$
-0.41	0.4589	0.31	0.3590	0.64	0.3049	-0.75	0.2466
.61	.4579	1.30	.3635	1.56	.3109	.21	.2471
1.53	.4623	2.27	.3737	2.58	.3249	1.15	.2481
2.53	.4738	3.28	.3901	3.57	.3371	2.14	.2501
3.51	.4876	4.27	.4103	4.55	.3511	3.10	.2579
6.54	.5478	7.30	.4645	7.56	.3800	6.05	.2797
11.73	.6664	12.45	.5257	12.64	.4170	11.05	.2971
17.13	.7411	17.65	.5554	17.77	.4292	16.15	.3059
22.58	.7951	22.98	.5506	23.13	.4064	21.44	.2867
27.53	.8281	27.93	.5105	28.01	.3691	26.26	.2633

$\left[M = 1.97\right]$

$R = 0.7 \times 10^6$		$R = 2.1 \times 10^6$		$R = 3.5 \times 10^6$		$R = 4.9 \times 10^6$		$R = 6.5 \times 10^6$		$R = 8.6 \times 10^6$	
α, deg	$C_{A,c}$	α, deg	$C_{A,c}$	α, deg	$C_{A,c}$	α, deg	$C_{A,c}$	α, deg	$C_{A,c}$	α, deg	$C_{A,c}$
0.28	0.3441	0.30	0.3453	0.31	0.3590	0.33	0.3675	0.36	0.3749	0.37	0.3806
1.20	.3423	1.25	.3501	1.30	.3635	1.34	.3728	1.36	.3797	1.46	.3862
2.12	.3571	2.19	.3583	2.27	.3737	2.35	.3835	2.43	.3896	2.54	.3944
3.04	.3708	3.18	.3762	3.28	.3901	3.39	.4000	3.52	.4070	3.68	.4127
4.00	.3880	4.13	.3964	4.27	.4103	4.41	.4196	4.56	.4257	4.77	.4313
6.84	.4560	7.08	.4547	7.30	.4645	7.54	.4718	7.79	.4775	8.17	.4824
11.70	.5350	12.07	.5185	12.45	.5257	12.84	.5315	13.29	.5364	13.89	.5403
16.69	.5553	17.17	.5524	17.65	.5554	18.15	.5562	18.72	.5576	19.48	.5584
21.88	.5313	22.44	.5471	22.98	.5506	23.56	.5490	24.24	.5428	25.10	.5397
26.66	.5071	27.29	.5174	27.93	.5105	28.57	.4960	29.32	.4919	30.31	.4869

[redacted]

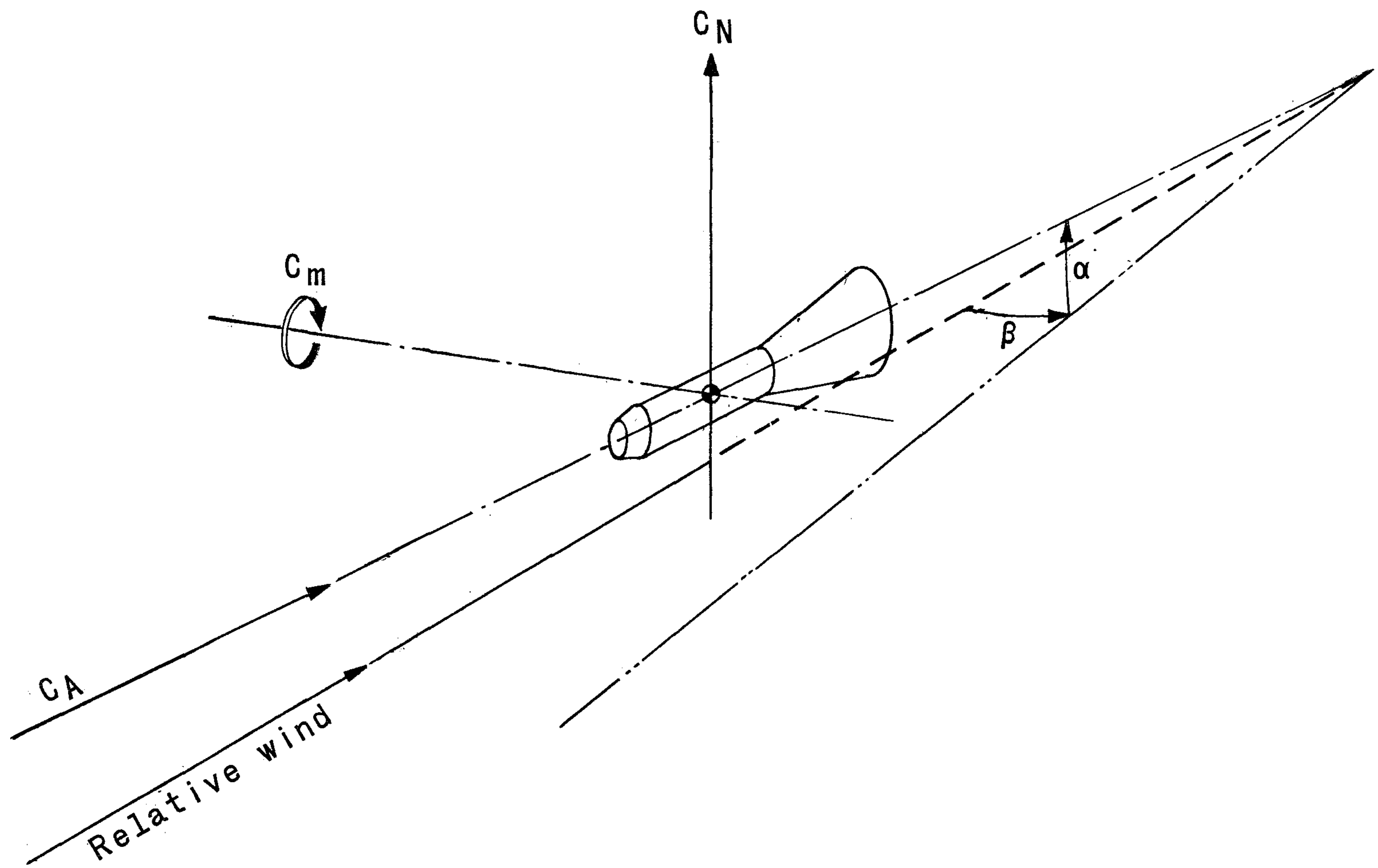

Figure 1.- Body axes system. (Arrows indicate positive direction.)

[redacted]

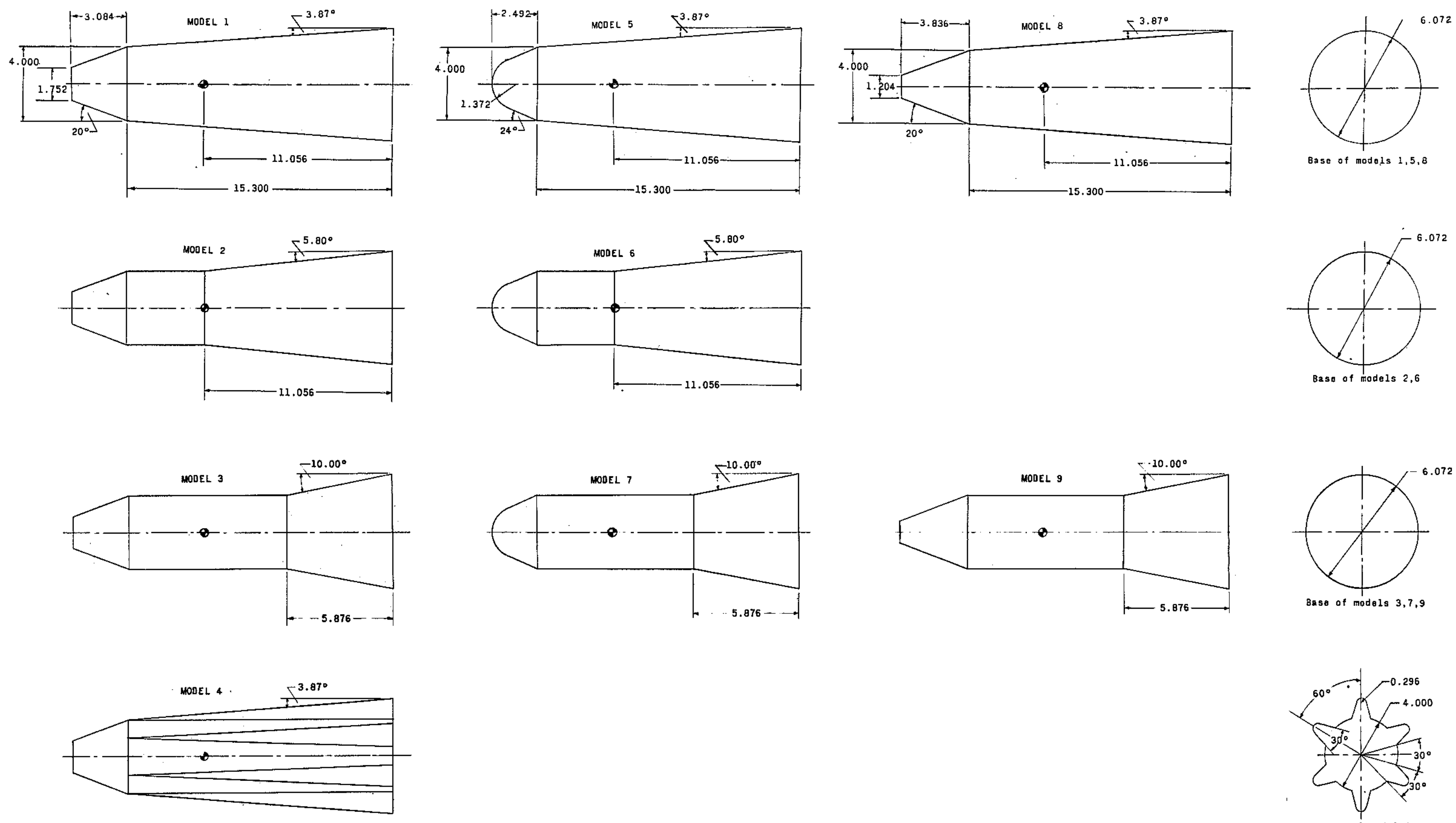

Figure 2.- Dimensions of models. (All dimensions in inches unless otherwise noted.)

[redacted]

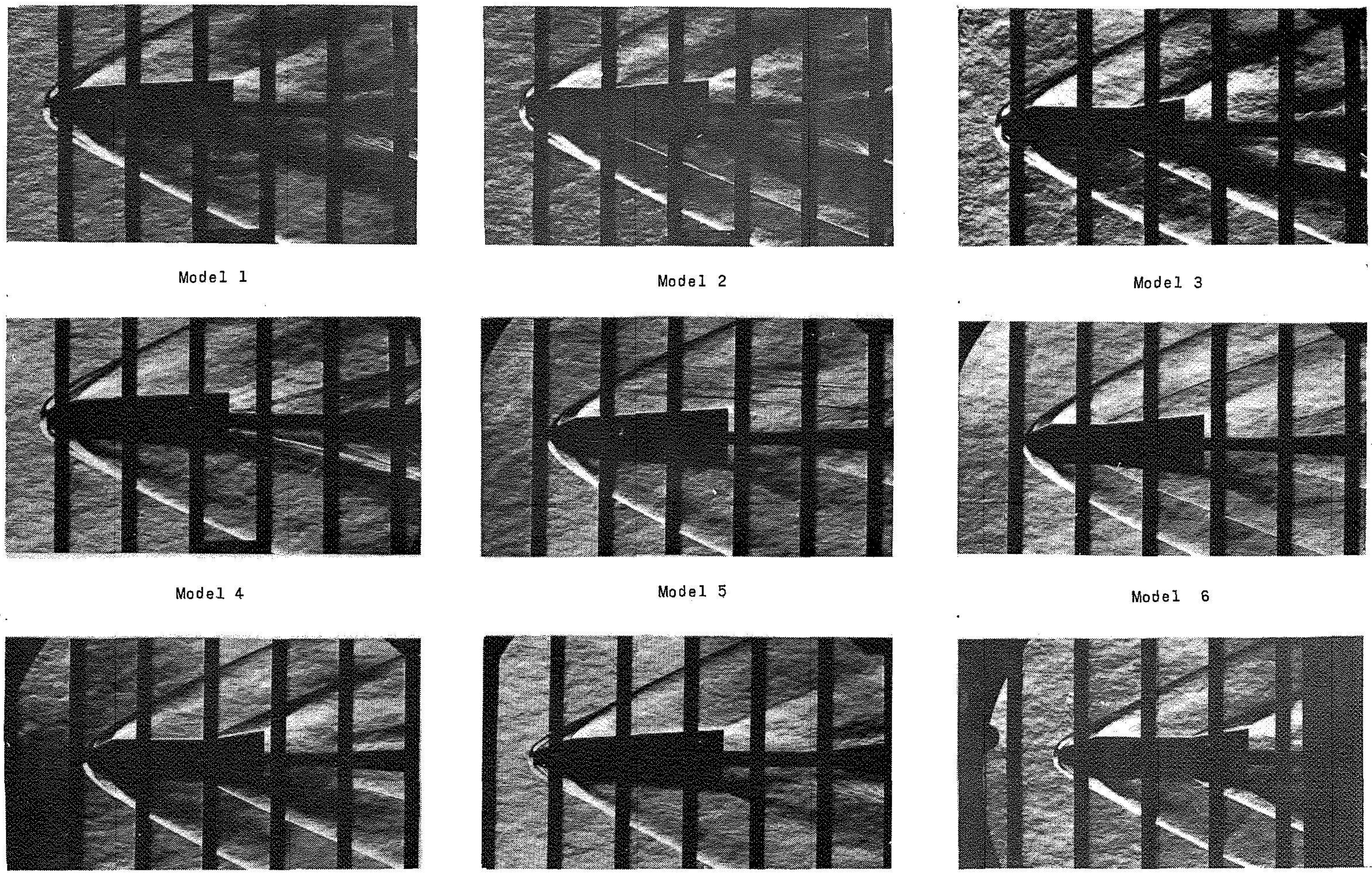

L-59-3032

Figure 3.- Typical schlieren photographs of all models at $M = 2.87$ and $\alpha \approx 0^{\circ}$.

[redacted]

[redacted]

L-356

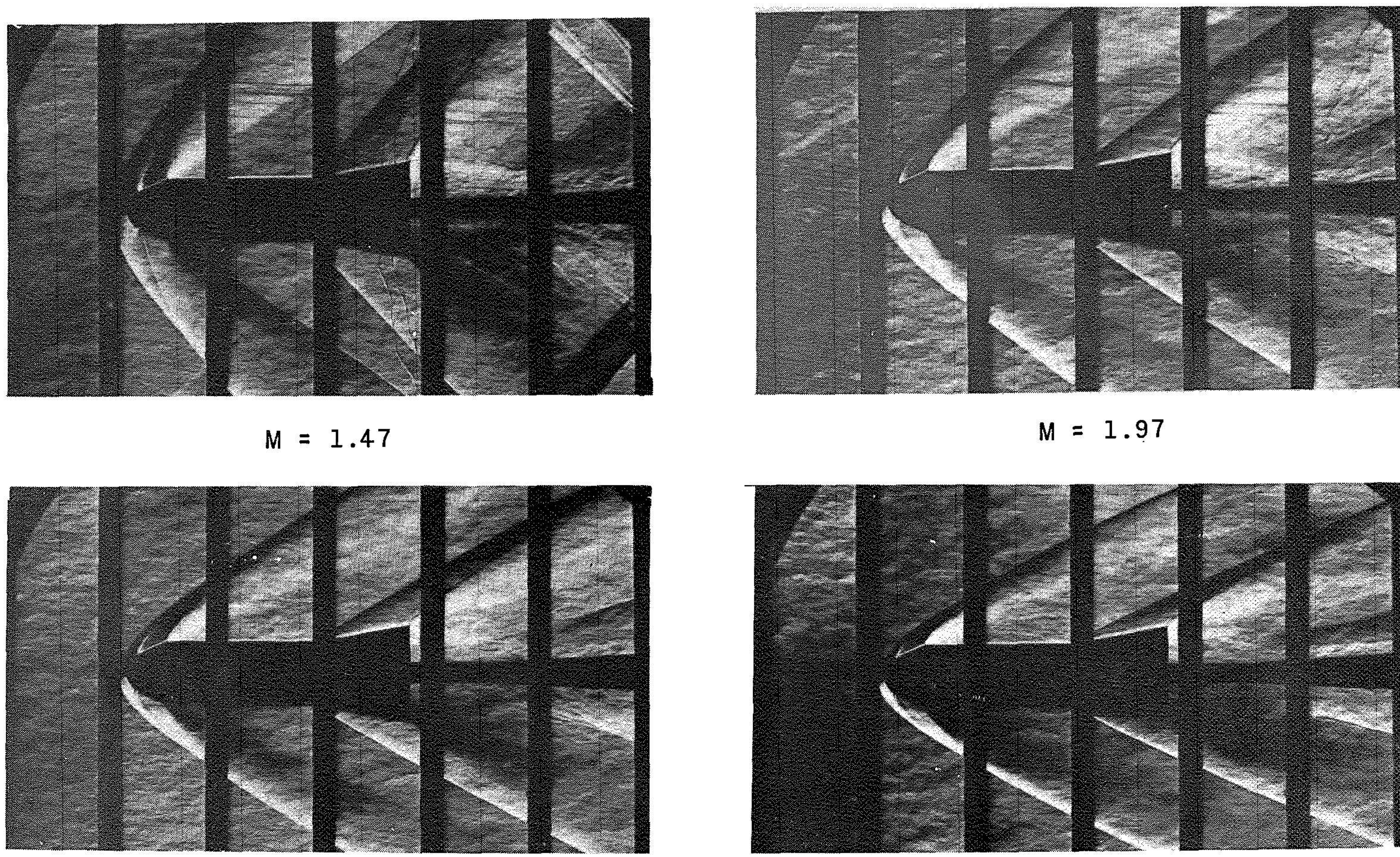

M = 1.47

M = 1.97

M = 2.36

M = 2.87

L-59-3033

Figure 4.- Typical schlieren photographs of model 7 at $R = 3.5 \times 10^6$ and $\alpha \approx 0^{\circ}$.

[redacted]

[redacted]

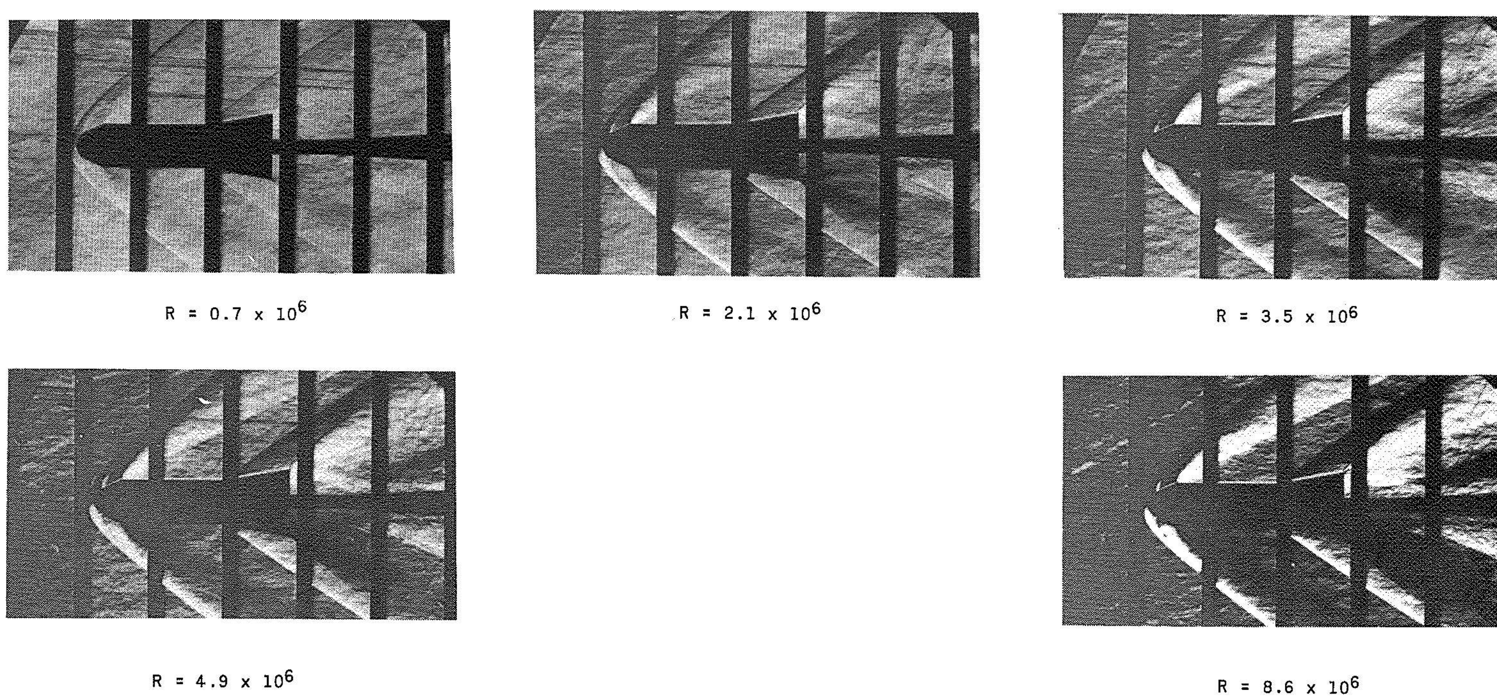

L-59-3034

Figure 5.- Typical schlieren photographs of model 7 at $M = 1.97$ and $\alpha \approx 0^\circ$.

[redacted]

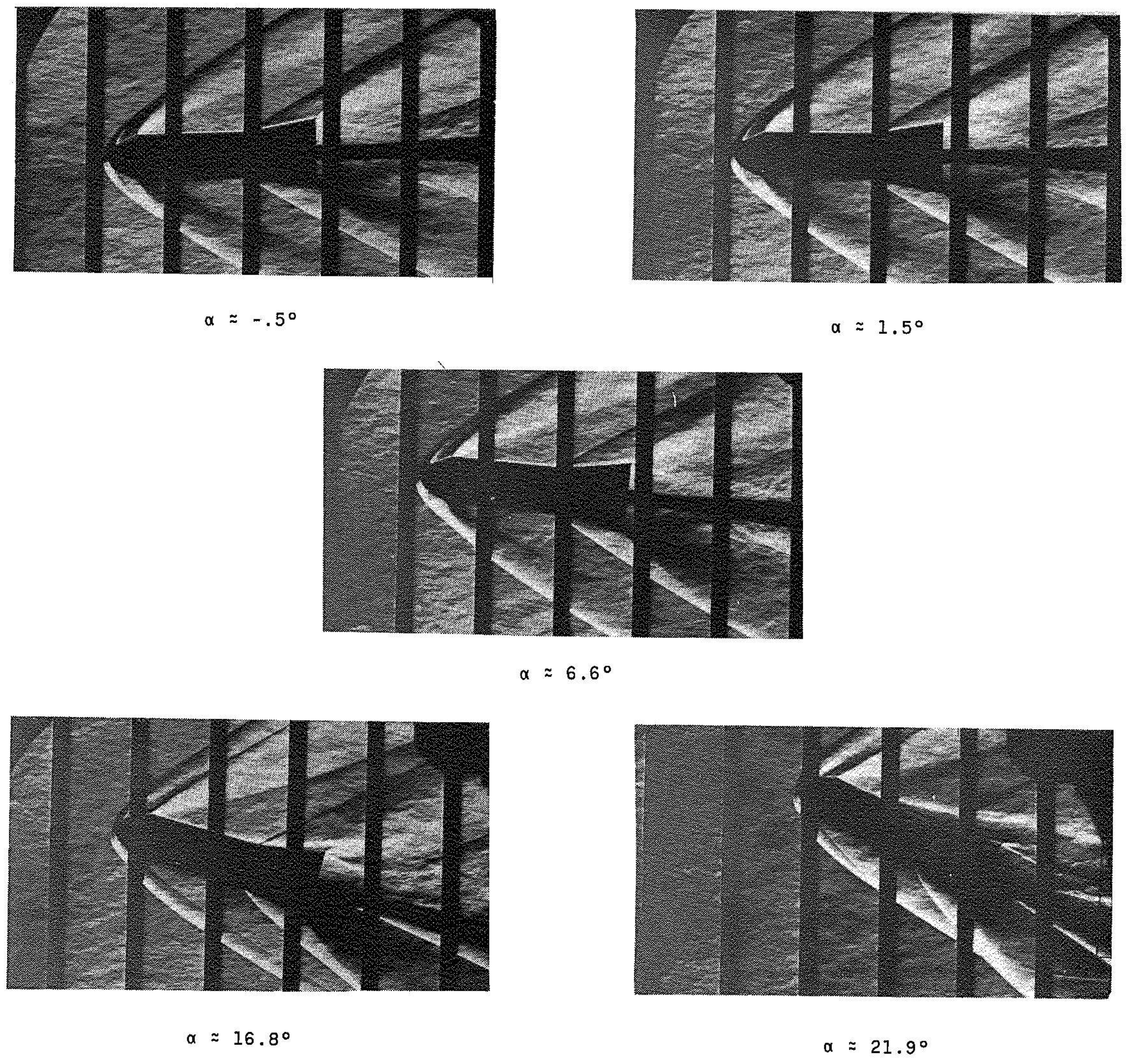

L-59-3035

Figure 6.- Typical schlieren photographs of model 7 through the angle-of-attack range at $M = 2.36$ and $R = 3.5 \times 10^6$.

[redacted]

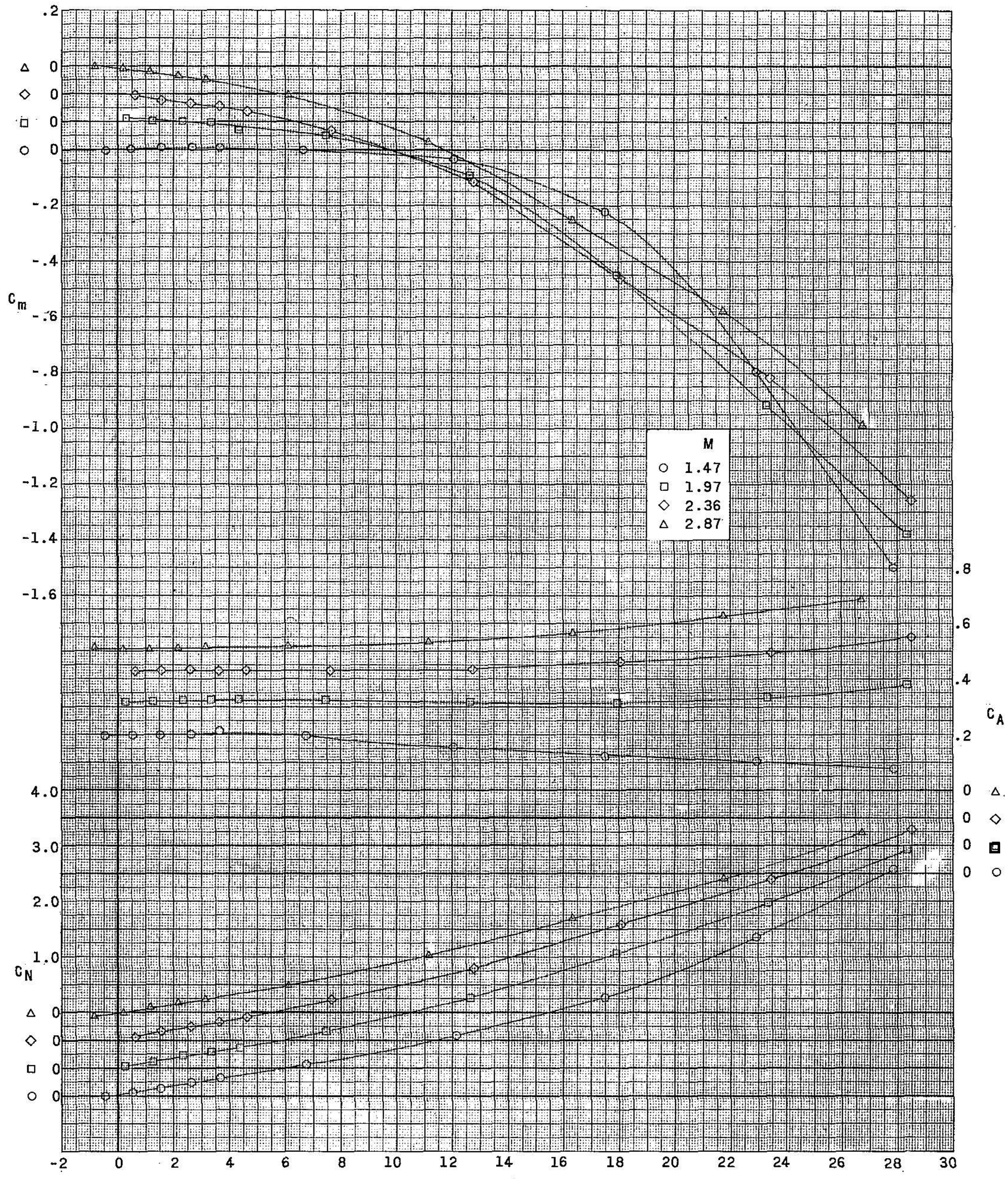

(a) Mach number effect. $R = 3.5 \times 10^6$.

Figure 7.- Aerodynamic characteristics of model 1 in pitch. $l_n/d_b = 0.51$; $l_f/d_b = 2.52$.

L-356

[redacted]

L-356

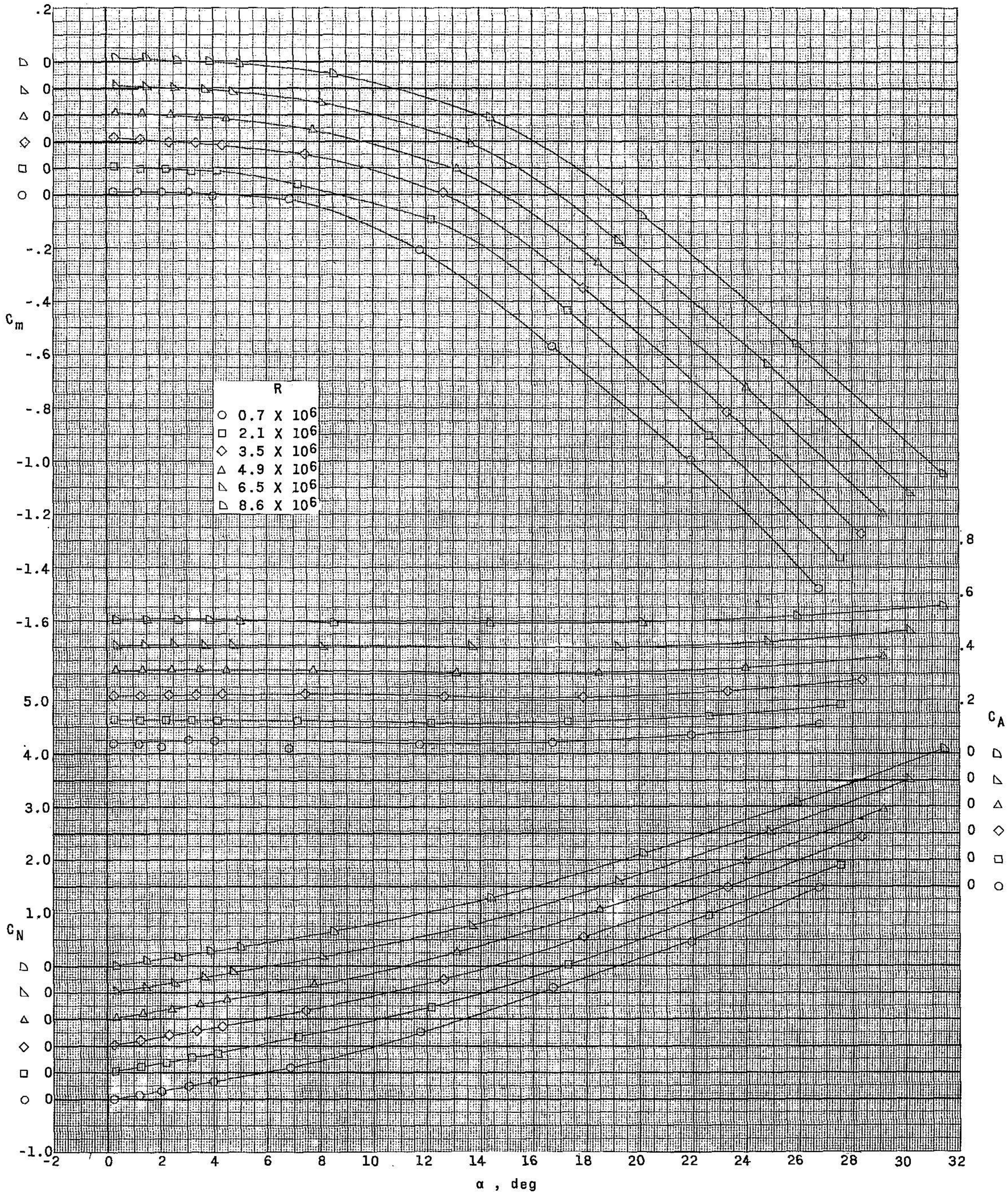

(b) Reynolds number effect. M = 1.97.

Figure 7.- Concluded.

[redacted]

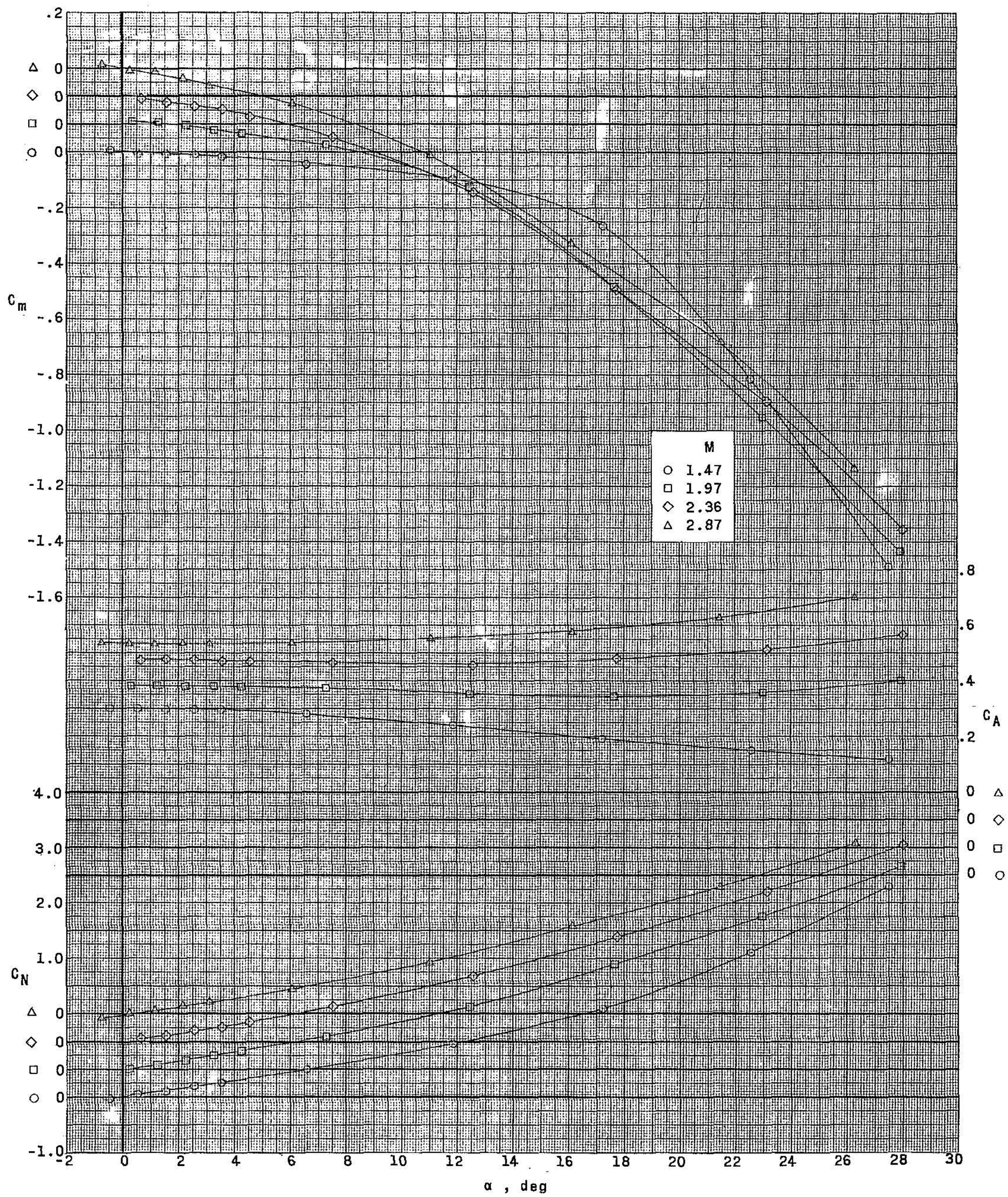

(a) Mach number effect. $R = 3.5 \times 10^6$.

Figure 8.- Aerodynamic characteristics of model 2 in pitch.
$l_n/d_b = 0.51$; $l_f/d_b = 1.82$.

L-356

[redacted]

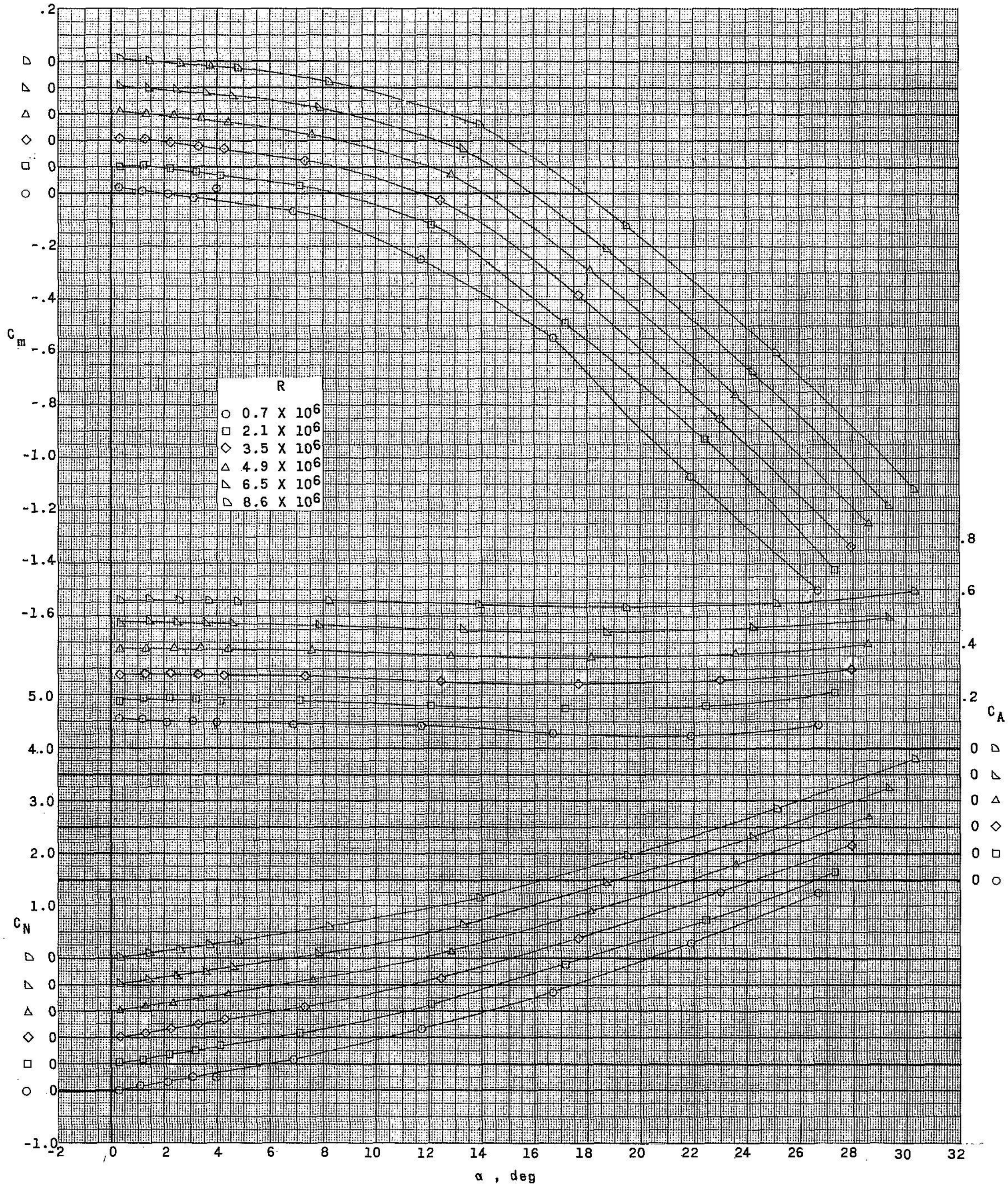

(b) Reynolds number effect. M = 1.97.

Figure 8.- Concluded.

[redacted]

[redacted]

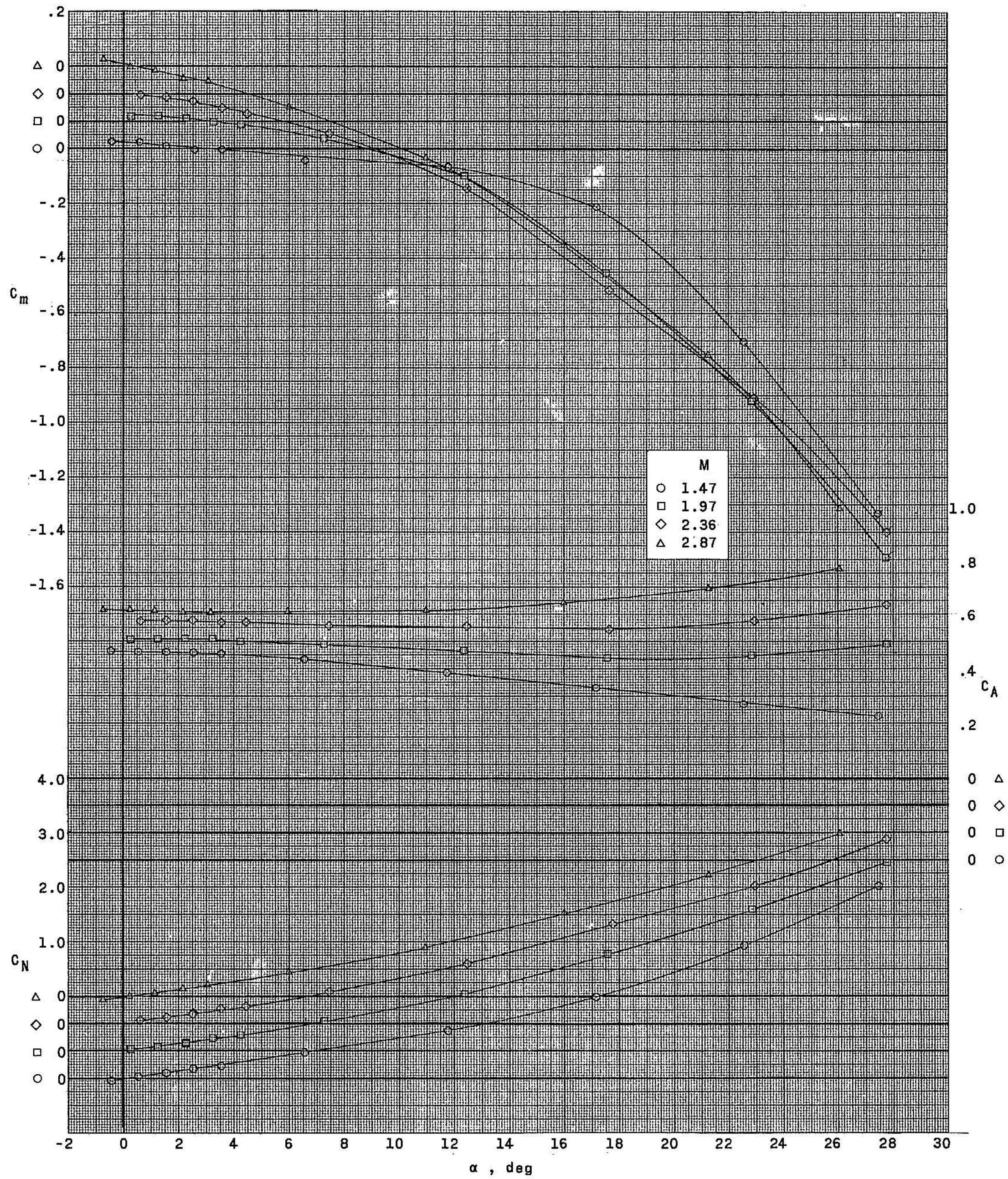

(a) Mach number effect. $R = 3.5 \times 10^6$.

Figure 9.- Aerodynamic characteristics of model 3 in pitch. $l_n/d_b = 0.51$; $l_f/d_b = 0.97$.

L-356

[redacted]

L-356

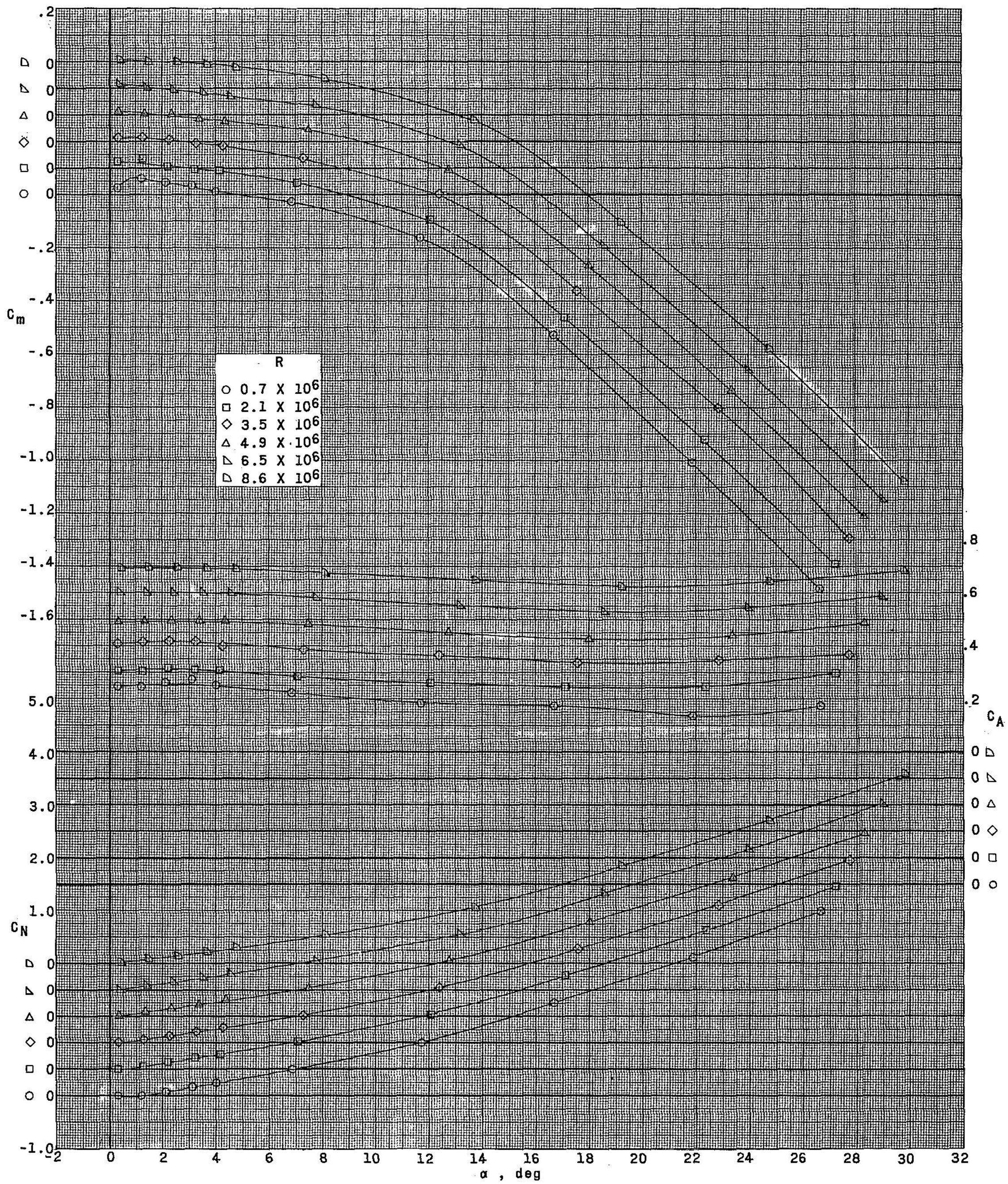

(b) Reynolds number effect. M = 1.97.

Figure 9.- Concluded.

[redacted]

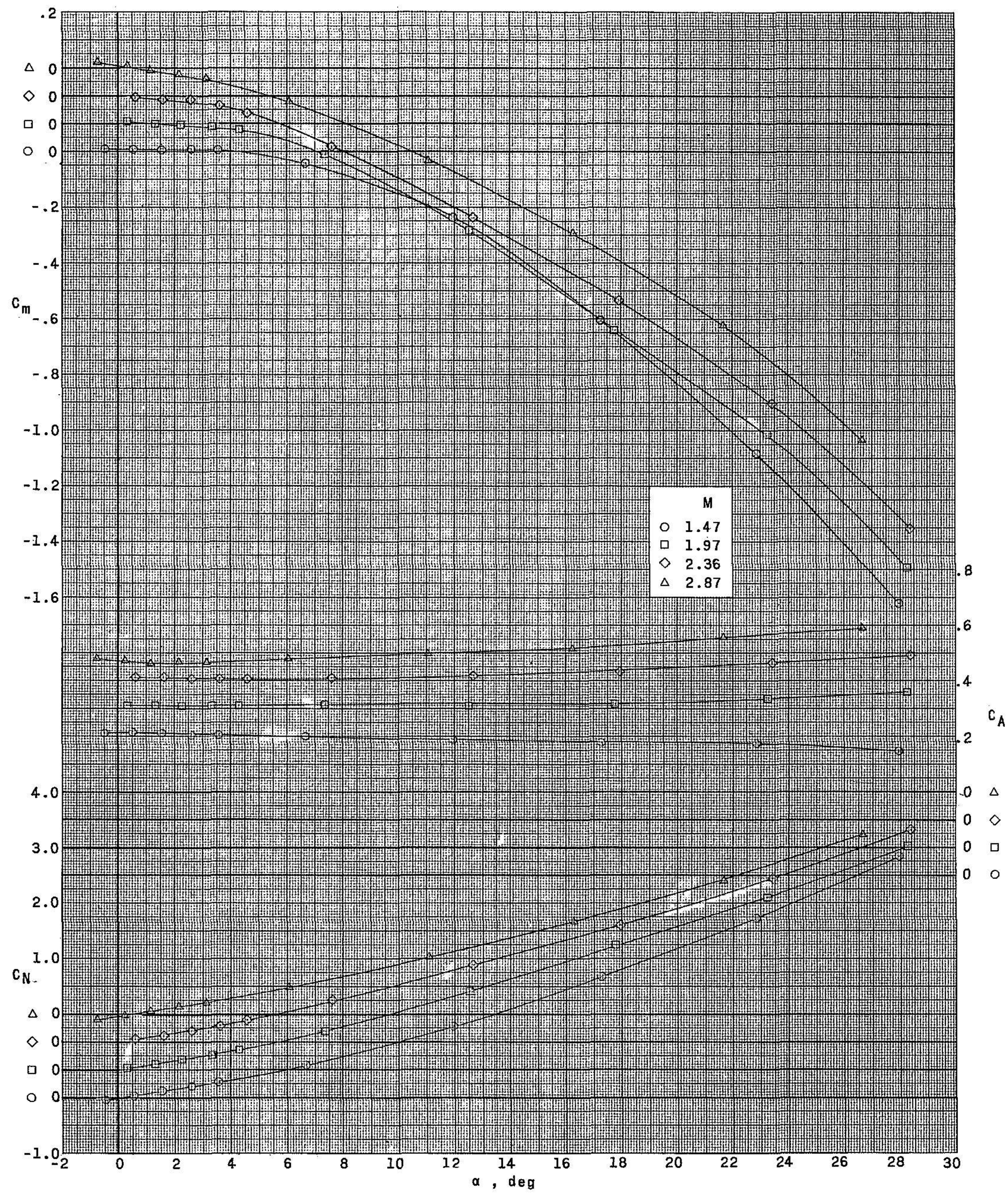

(a) Mach number effect. $R = 3.5 \times 10^6$.

Figure 10.- Aerodynamic characteristics of model 4 in pitch. $l_n/d_b = 0.51$; $l_f/d_b = 2.52$.

L-556

[redacted]

L-356

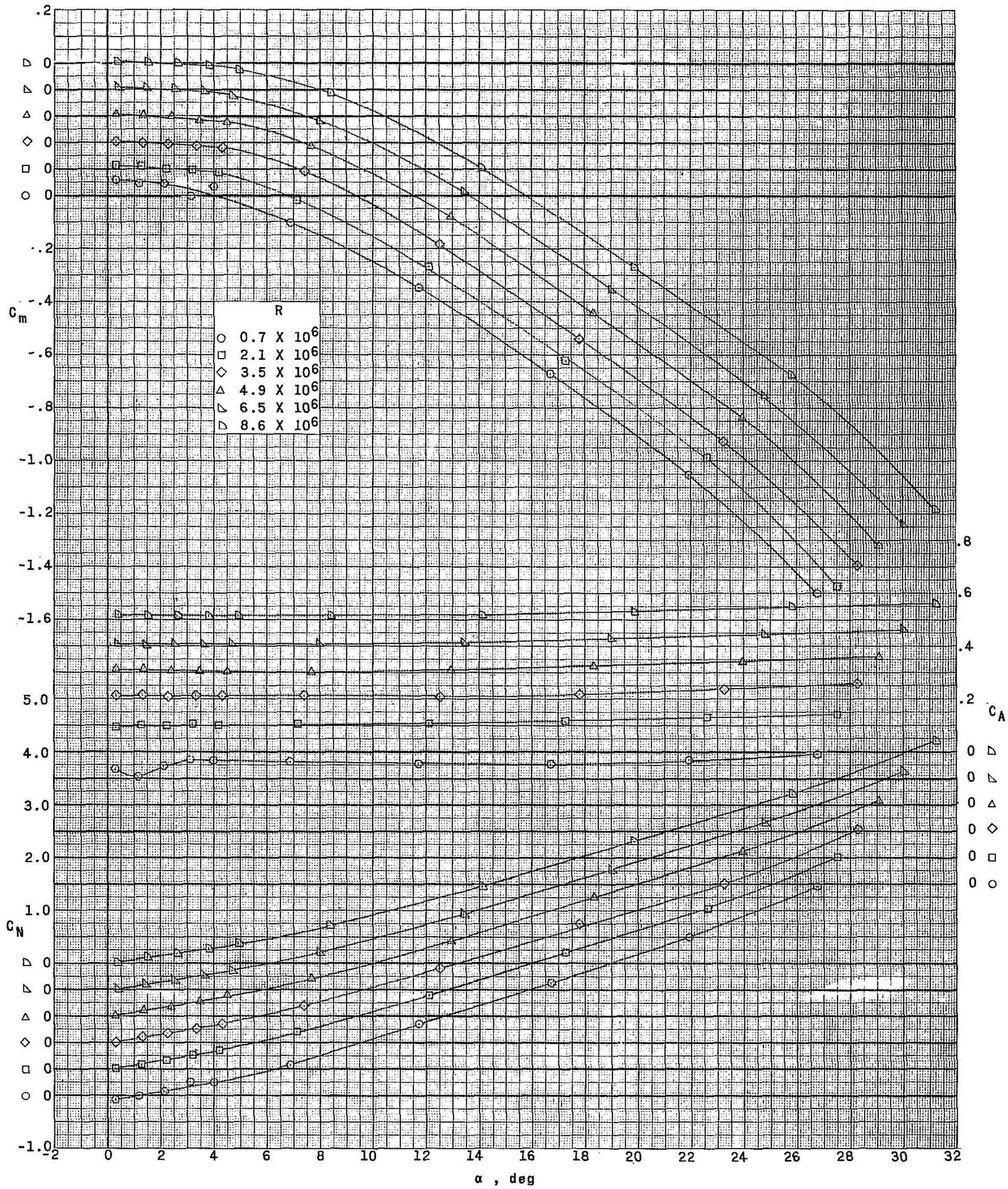

(b) Reynolds number effect. $M = 1.97$.

Figure 10.- Concluded.

[redacted]

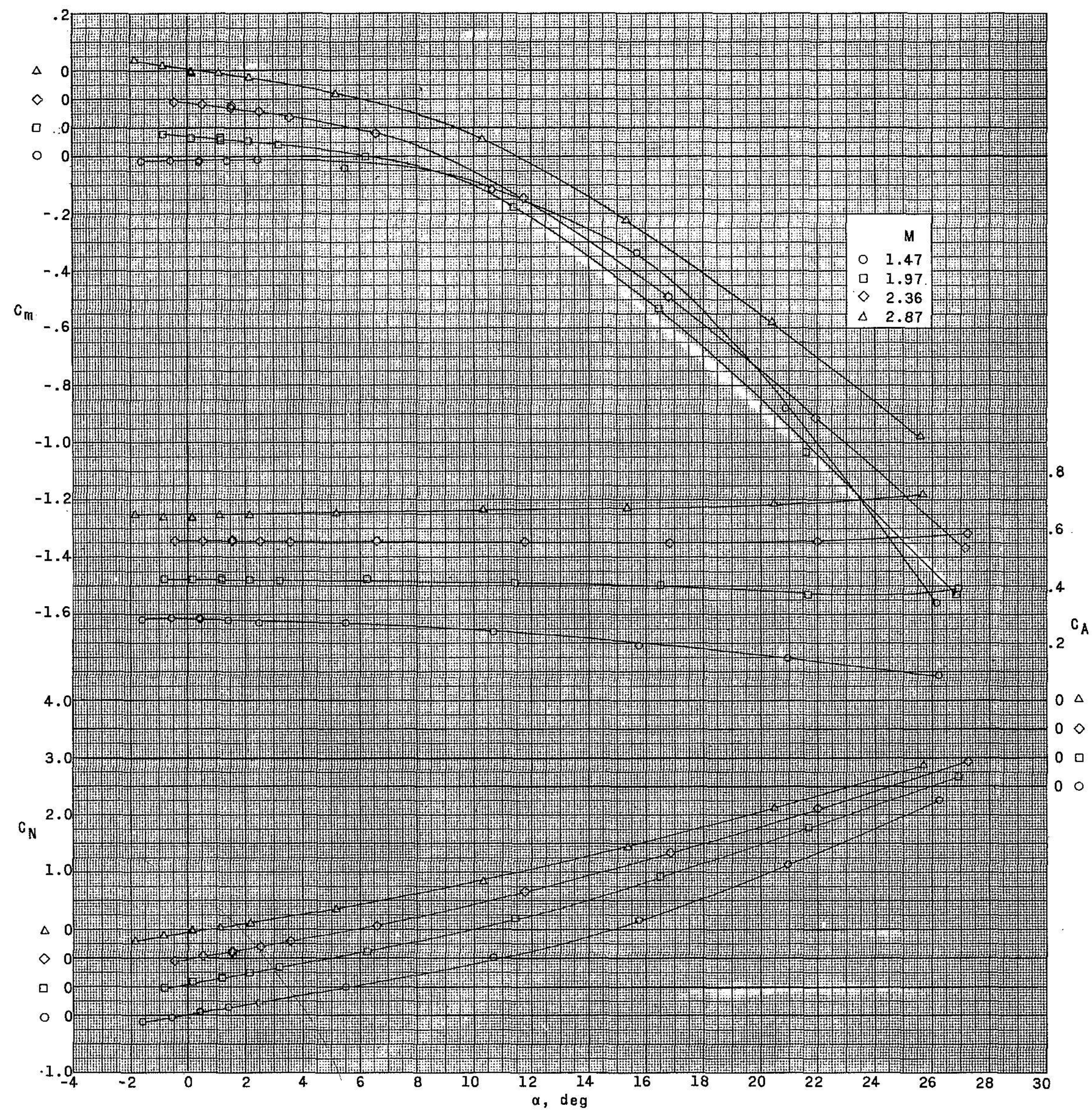

L-356

(a) Mach number effect. $R = 3.5 \times 10^6$.

Figure 11.- Aerodynamic characteristics of model 5 in pitch. Round nose; $l_n/d_b = 0.41$; $l_f/d_b = 2.52$.

[redacted]

L-356

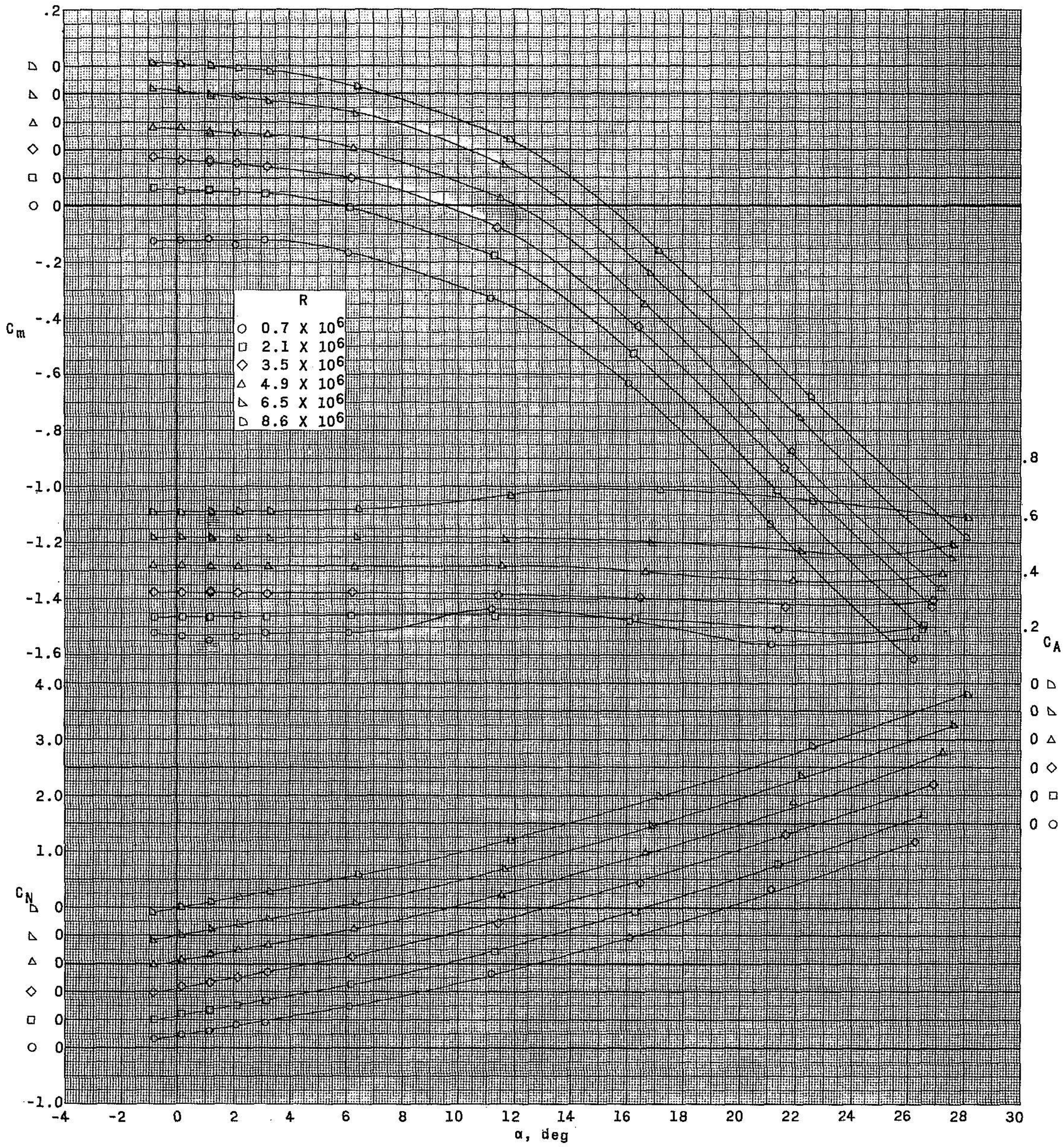

(b) Reynolds number effect. M = 1.97.

Figure 11.- Concluded.

[redacted]

L-356

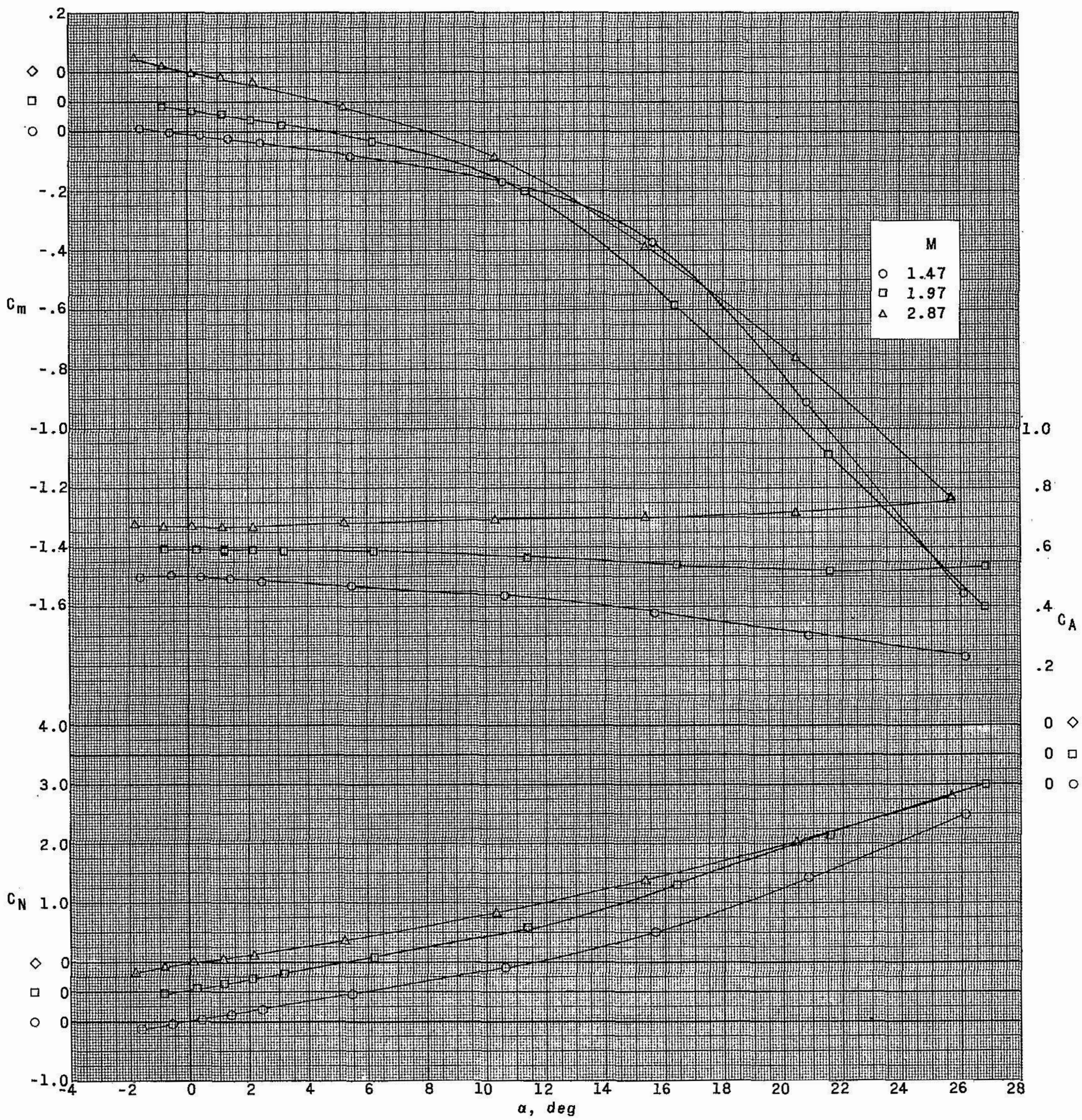

Figure 12.- Aerodynamic characteristics of model 6 in pitch. Round nose; $R = 3.5 \times 10^6$; $l_n/d_b = 0.41$; $l_f/d_b = 1.82$.

[redacted]

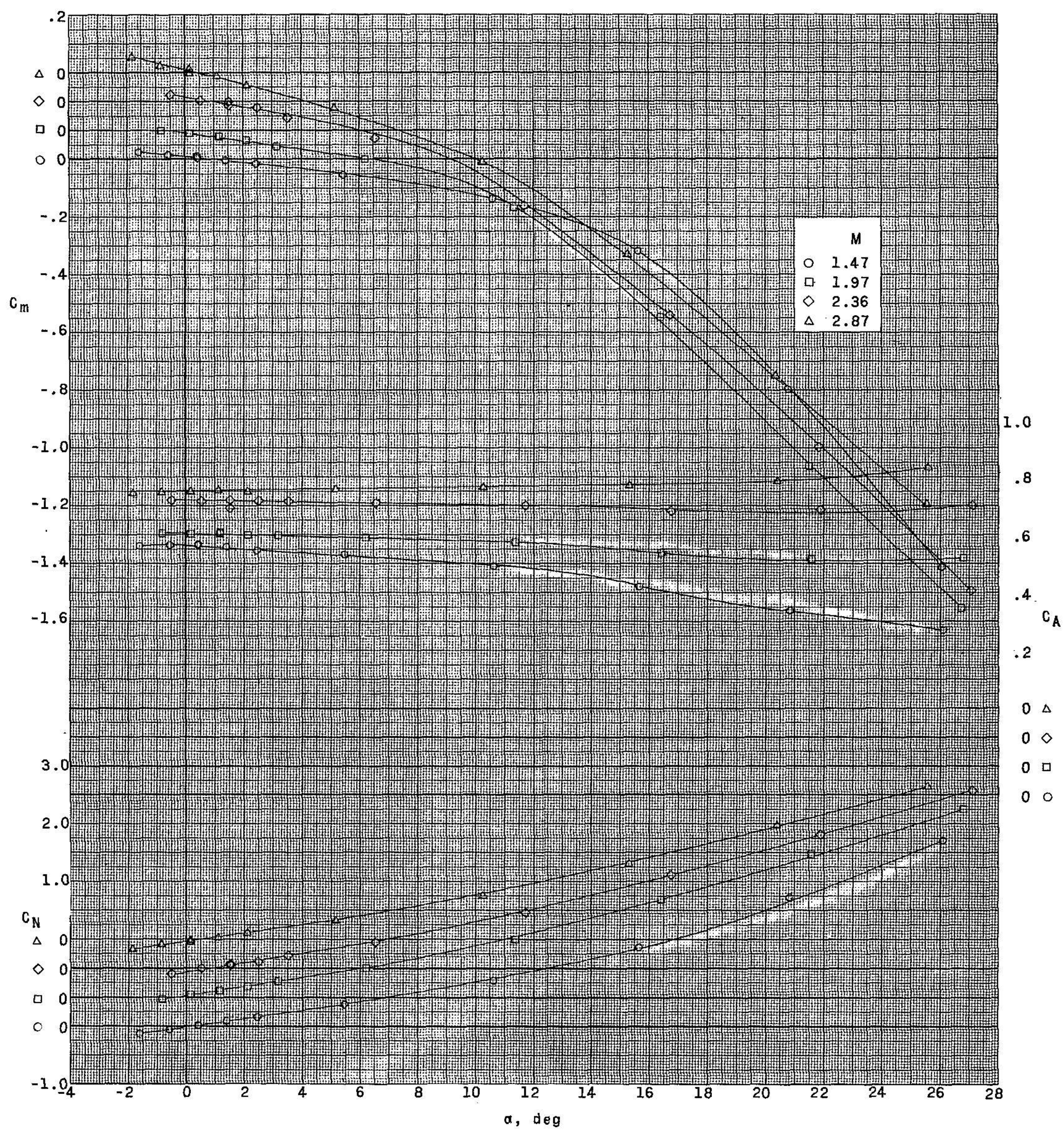

(a) Mach number effect. $R = 3.5 \times 10^6$.

Figure 13.- Aerodynamic characteristics of model 7 in pitch. Round nose; $l_n/d_b = 0.41$; $l_f/d_b = 0.97$.

[redacted]

[redacted]

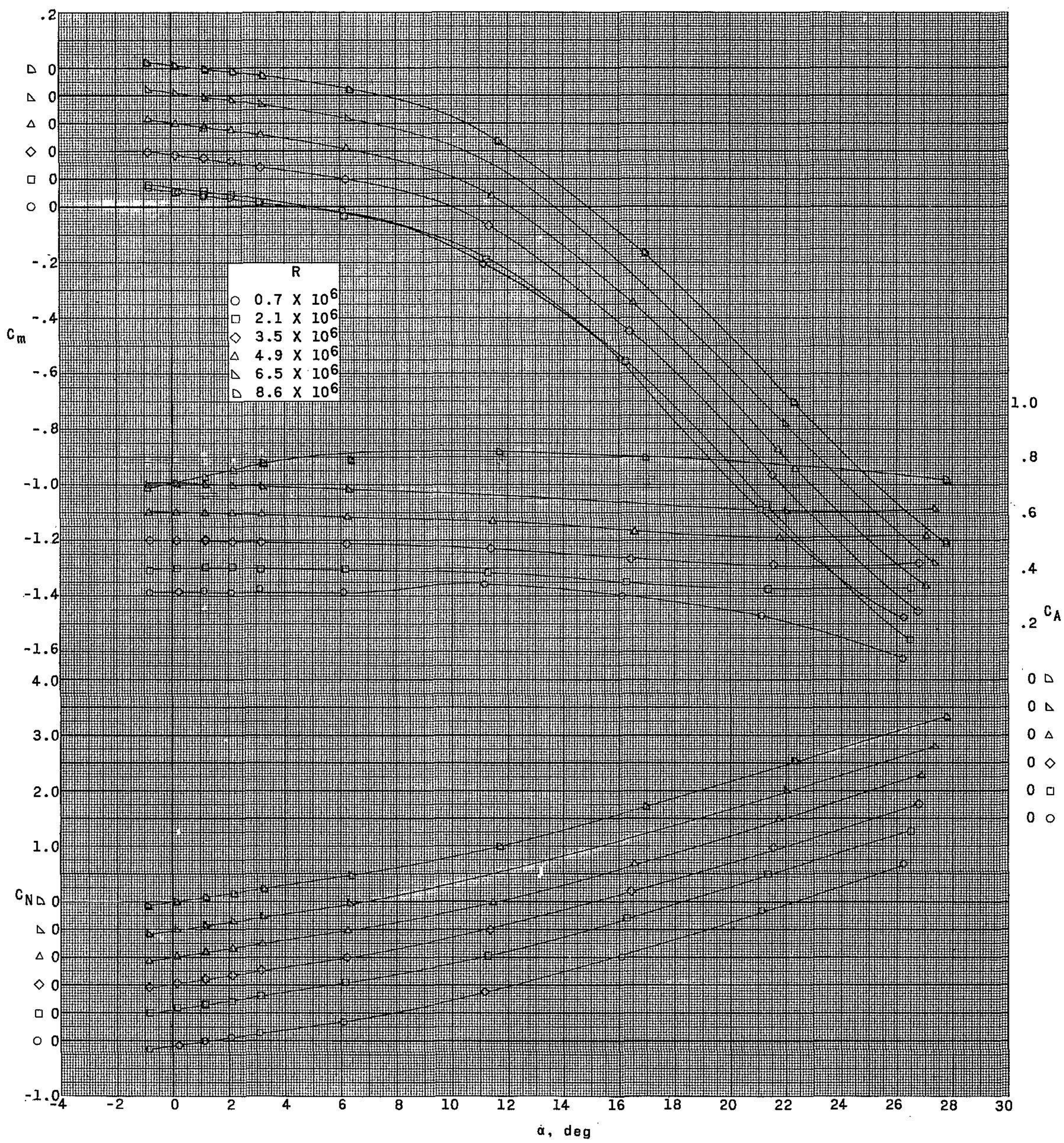

(b) Reynolds number effect. M = 1.97.

Figure 13.- Concluded.

L-356

[redacted]

L-556

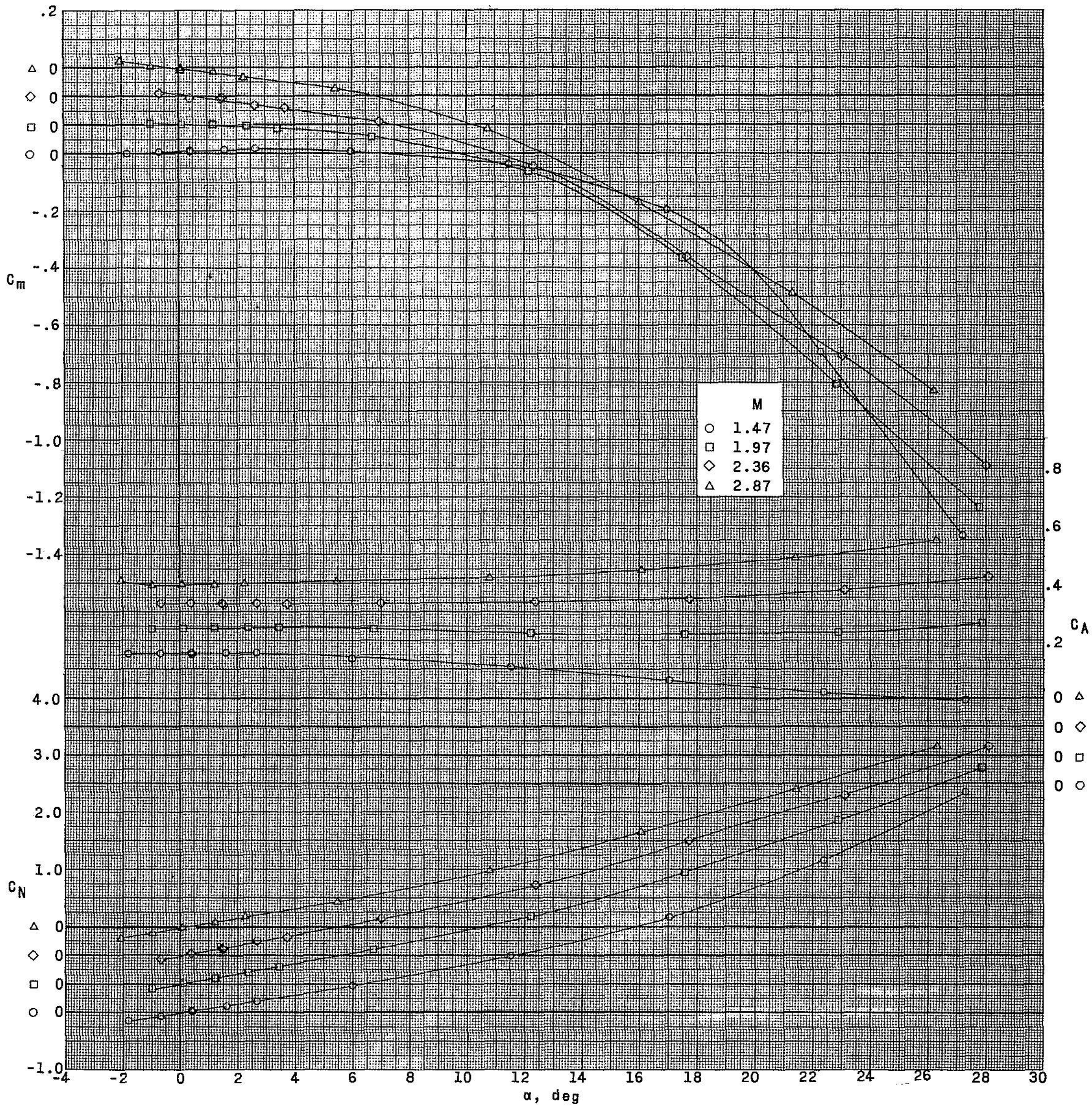

(a) Mach number effect. $R = 3.5 \times 10^6$.

Figure 14.- Aerodynamic characteristics of model 8 in pitch.
$l_n/d_b = 0.63$; $l_f/d_b = 2.52$.

[redacted]

L-356

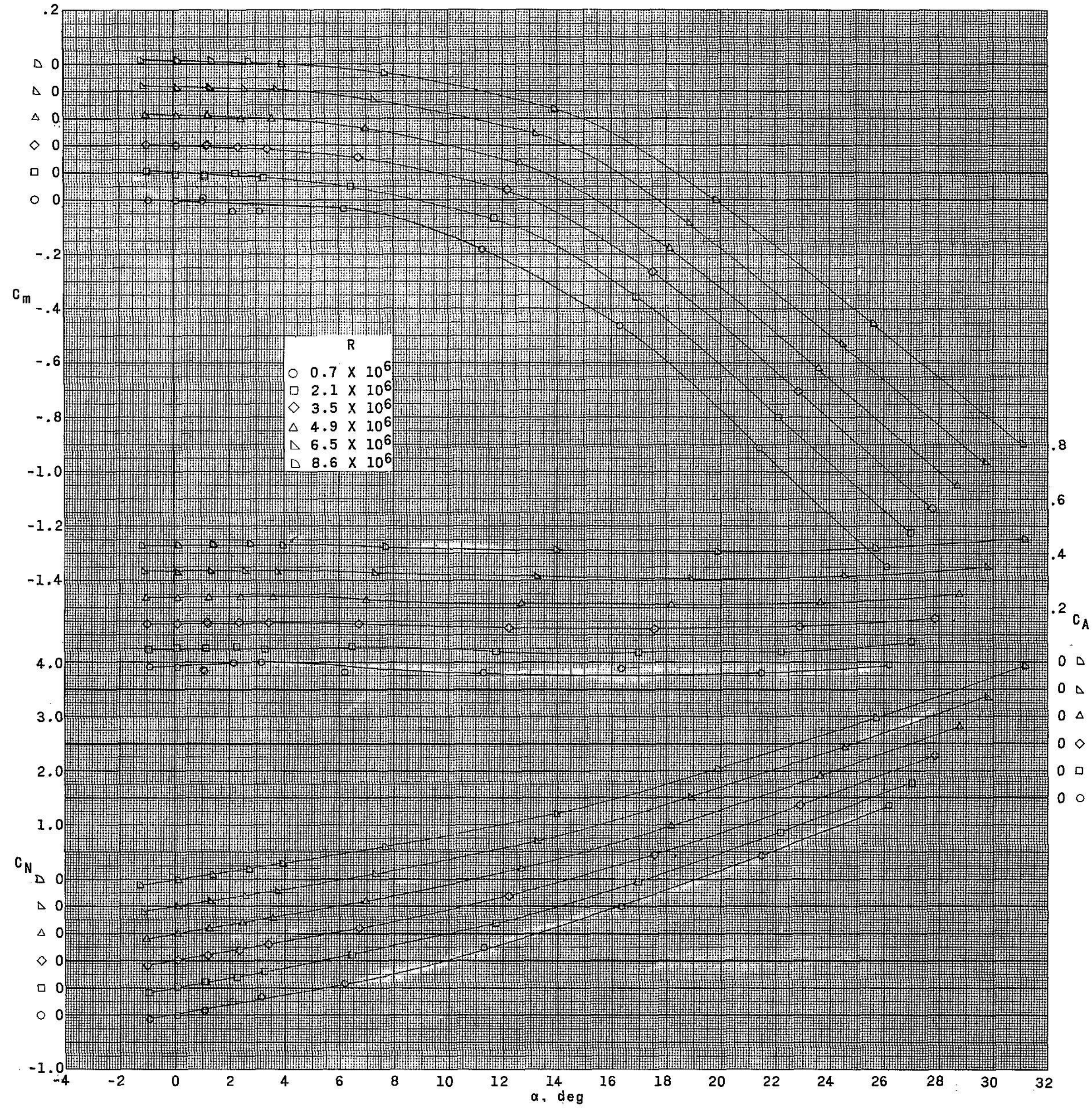

(b) Reynolds number effect. M = 1.97.

Figure 14.- Concluded.

[redacted]

[redacted]

L-356

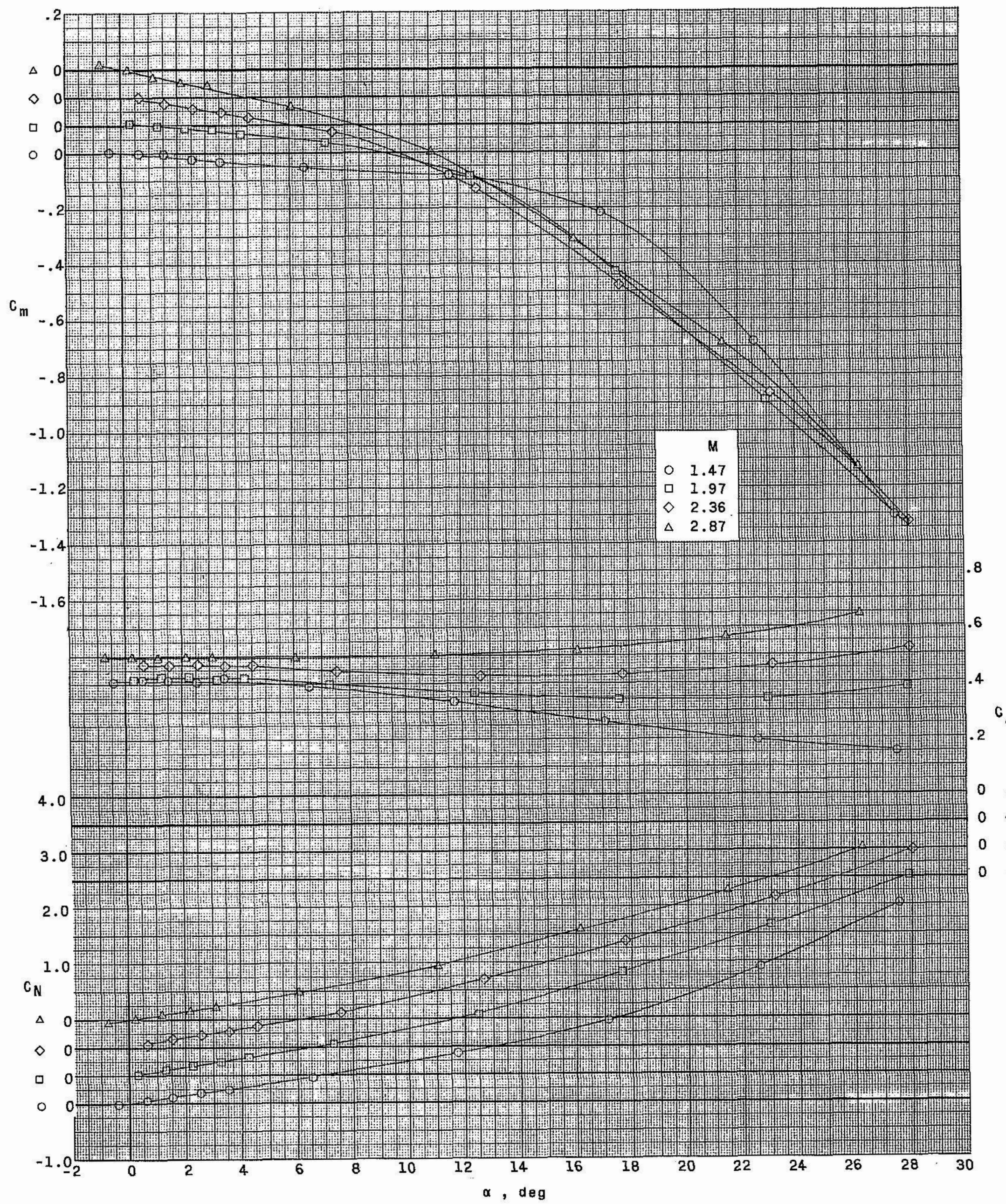

(a) Mach number effect. $R = 3.5 \times 10^6$.

Figure 15.- Aerodynamic characteristics of model 9 in pitch. $l_n/d_b = 0.63$; $l_f/d_b = 0.97$.

[redacted]

[redacted]

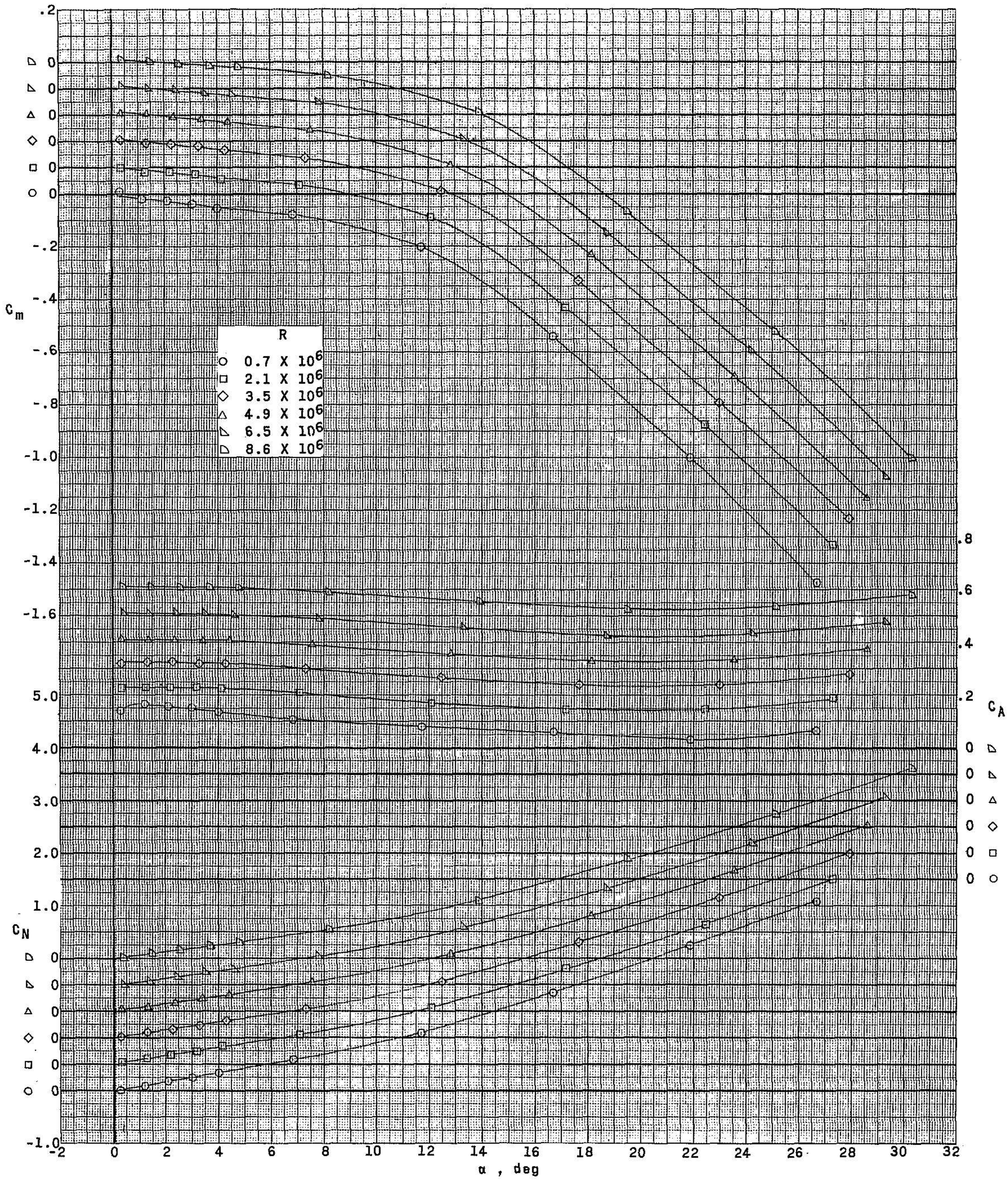

L-356

(b) Reynolds number effect. M = 1.97.

Figure 15.- Concluded.

[redacted]

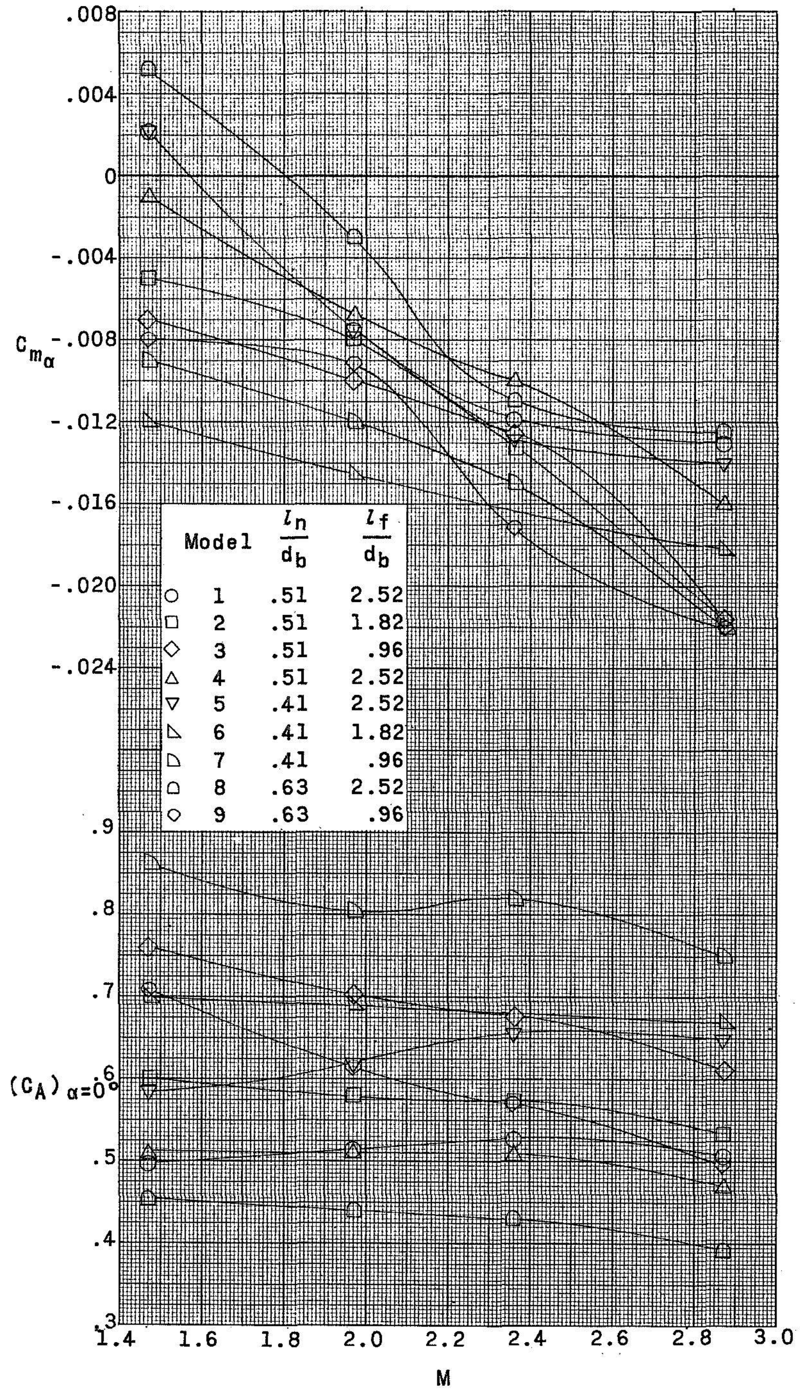

Figure 16.- Summary of longitudinal stability characteristics of models tested. $R = 3.5 \times 10^6$.